nature chemistry

SUPPLEMENTARY INFORMATION

DOI: 10.1038/NCHEM.2783

In the format provided by the authors and unedited.

Enantioselective, intermolecular benzylic C–H amination catalysed by an engineered iron-haem enzyme

Christopher K. Prier,[†] Ruijie K. Zhang,[†] Andrew R. Buller, Sabine Brinkmann-Chen, and Frances H. Arnold*

Division of Chemistry and Chemical Engineering, California Institute of Technology, 1200 East California Boulevard, MC 210-41, Pasadena, CA 91125, United States

Email: frances@cheme.caltech.edu

This PDF includes:

Experimental Procedures

General. Unless otherwise noted, all chemicals and reagents were obtained from commercial suppliers (Sigma-Aldrich, VWR, Alfa Aesar) and used without further purification. Silica gel chromatography was carried out using AMD Silica Gel 60, 230-400 mesh. ^{1}H and ^{13}C NMR spectra were recorded on a Varian Inova 300 MHz or 500 MHz, or Bruker Prodigy 400 MHz instrument, in $CDCl_3$ and are referenced to residual protio solvent signals. Data for ^{1}H NMR are reported as follows: chemical shift (δ ppm), multiplicity (s = singlet, d = doublet, t = triplet, q = quartet, p = pentet, m = multiplet, dd = doublet of doublets, dt = doublet of triplets, ddd = doublet of doublet of doublets), coupling constant (Hz), integration. Sonication was performed using a Qsonica Q500 sonicator. High-resolution mass spectra were obtained at the California Institute of Technology Mass Spectral Facility. Synthetic reactions were monitored using thin layer chromatography (Merck 60 gel plates) using a UV-lamp for visualization. Substrates were purchased from commercial suppliers. Tosyl azide was prepared according to de Nanteuil and Waser.[1]

Chromatography. Analytical high-performance liquid chromatography (HPLC) was carried out using an Agilent 1200 series instrument and a Kromasil 100 C18 column (4.6 x 50 mm, 5 μm) with water and acetonitrile as the mobile phase. Semi-preparative HPLC was performed using an Agilent XDB-C18 column (9.4 x 250 mm, 5 μm) with water and acetonitrile as the mobile phase. Analytical chiral HPLC was conducted using a supercritical fluid chromatography (SFC) system with isopropanol and liquid CO_2 as the mobile phase. Product enantiomers were separated using a Chiralpak AS column (4.6 x 150 mm, 5 μm) from Chiral Technologies Inc.

Cloning and site-directed mutagenesis. pET22b(+) was used as a cloning and expression vector for all enzymes described in this study. Site-directed mutagenesis was performed using a modified QuikChange™ mutagenesis protocol.[2] The PCR products were digested with *Dpn*I, gel purified, and the gaps were repaired using Gibson Mix™.[3] The ligation mixture was used to directly transform *E. coli* strain BL21 *E. cloni* (Lucigen).

Determination of P411 concentration. The concentration of P411 enzymes in whole cell experiments was determined from ferrous carbon monoxide binding difference spectra using the previously reported extinction coefficient for serine-ligated enzymes (ε = 103,000 M^{-1} cm^{-1}).[4] The concentration of purified P411 enzymes was determined by quantifying the amount of free hemin present using the pyridine/hemochrome assay and the published extinction coefficient (ε = 191,500 M^{-1} cm^{-1}).[5]

Expression and amination bioconversions using whole cells. *E. coli* BL21 *E. cloni* cells carrying a plasmid encoding a P411 variant were grown overnight in 5 mL Luria-Bertani medium with 0.1 mg/mL ampicillin (LB_{amp}, 37 ºC, 250 rpm). The preculture was used to inoculate 45 mL of Hyperbroth (HB) medium (prepared from AthenaES© powder, 0.1 mg/mL ampicillin) in a 125-mL Erlenmeyer flask; this culture was incubated at 37 ºC, 230 rpm for 2 h. Cultures were then cooled on ice (20 min), and expression was induced with 0.5 mM IPTG and 1.0 mM 5-aminolevulinic acid (final concentrations). Expression was conducted at room temperature (23 ºC), at 130 rpm, for 16–18 h. Cultures were then centrifuged (2,600 x g, 10 min, 4 ºC), and the pellets were resuspended to an OD_{600} of 30 in M9-N minimal media (no nitrogen). Aliquots of the cell suspension (4 mL) were used to determine the P411 expression level after lysis by sonication.

For amination bioconversions, the cells (OD_{600} of 30 in M9-N media) were degassed by sparging with argon in sealed 6-mL crimp vials for at least 40 minutes. Separately, a glucose solution (250 mM in M9-N) was degassed by sparging with argon for at least 10 minutes. An oxygen depletion system (20 μL of a stock solution containing 14,000 U/mL catalase and 1,000 U/mL glucose oxidase in 0.1 M KPi, pH 8.0) was added to 2-mL crimp vials. All solutions were uncapped and transferred into an anaerobic chamber. Resuspended cells (320 μL) were added to the vials, followed by glucose (40 μL, 250 mM in M9-N), alkane (10 μL of a DMSO stock), and tosyl azide (10 μL of a DMSO stock). Final concentrations were typically 2.5–5.0 mM alkane, 5.0 mM tosyl azide, and 25 mM glucose; final reaction volume was 400 μL. The vials were sealed, removed from the anaerobic chamber, and shaken at room temperature and 40 rpm for 16–20 h. Reactions under aerobic conditions were performed by combining resuspended cells (320 μL), glucose (40 μL, 250 mM in M9-N), oxygen depletion system (20 μL, or 20 μL M9-N), alkane (10 μL, 200 mM in DMSO), and tosyl azide (10 μL, 200 mM in DMSO) on the benchtop,

without any argon sparging (final reaction volume 400 μL). The reactions were quenched by addition of acetonitrile (400 μL) and internal standard (10 μL of a DMSO stock). This mixture was then transferred to a microcentrifuge tube and centrifuged at 20,000 x g for 10 minutes. The supernatant was transferred to a vial and analyzed by HPLC.

Reaction screening in 96-well plate format. Site-saturation libraries were generated employing the "22c-trick" method.[2] *E. coli* libraries were cultured in LB_{amp} (300 μL/well) at 37 ºC, 220 rpm and 80% relative humidity overnight. Hyperbroth medium (1000 μL/well, 0.1 mg/mL ampicillin) was inoculated with the preculture (50 μL/well) and incubated at 37 ºC, 220 rpm, 80% humidity for 3 h. The plates were cooled on ice for 30 minutes, and then expression was induced with 0.5 mM IPTG and 1.0 mM 5-aminolevulinic acid (final concentrations). Expression was conducted at 20 ºC and 120 rpm for 24 h. The cells were pelleted (3,000 x g, 5 min, 4 ºC) and resuspended in the oxygen depletion system (20 μL/well). The 96-well plate was then transferred to an anaerobic chamber. In the anaerobic chamber, argon-sparged reaction buffer (50 mM glucose in M9-N, 300 μL/well) was added, followed by the alkane (10 μL/well, 200 mM in DMSO) and tosyl azide (10 μL/well, 200 mM in DMSO). The plate was sealed with an aluminum foil, removed from the anaerobic chamber, and shaken at 40 rpm. After 16–20 h, the seal was removed and acetonitrile (400 μL/well) and internal standard (10 μL/well of a DMSO stock) were added. The wells were mixed, the plate was centrifuged (5,000 x g, 10 min), and the supernatant was filtered through an AcroPrep 96-well filter plate (0.2 μm) into a shallow-well plate for HPLC analysis.

Protein purification. *E. coli* BL21 *E. cloni* cells carrying a plasmid encoding a P411 variant were grown overnight in 25 mL LB_{amp} (37 ºC, 250 rpm). Hyperbroth medium (630 mL, 0.1 mg/mL ampicillin) in a 1-L flask was inoculated with 25 mL of the preculture and incubated at 37 ºC and 230 rpm for 2.5 h (to OD_{600} ca. 1.8). Cultures were then cooled on ice (30 min) and induced with 0.5 mM IPTG and 1.0 mM 5-aminolevulinic acid (final concentrations). Expression was conducted at 23 ºC, 130 rpm, for 16–20 h. Cultures were then centrifuged (5,000 x g, 8 min, 4 ºC) and the cell pellets frozen at –20 ºC. For purification, frozen cells from two such cultures were resuspended in buffer A (25 mM tris, 20 mM imidazole, 100 mM NaCl, pH 7.5, 4 mL/g of cell wet weight), loaded with hemin (1 mg/gram wet cell weight) and powdered DNaseI, and

lysed by sonication. To pellet cell debris, lysates were centrifuged (20,000 x g, 20 min, 4 ºC). Proteins were expressed in a construct containing a 6x-His tag and purified using a nickel NTA column (1 mL HisTrap HP, GE Healthcare, Piscataway, NJ) using an AKTA or AKTAxpress purifier FPLC system (GE healthcare). P411 enzymes were eluted with a linear gradient from 100% buffer A to 100% buffer B (25 mM tris, 300 mM imidazole, 100 mM NaCl, pH 7.5) over 10 column volumes.

Proteins used for crystallography were subjected to an additional ion-exchange purification step. For these proteins, fractions were pooled and subjected to three exchanges of anion exchange buffer A (25 mM tris-HCl, pH 7.5) using centrifugal spin filters (10 kDa molecular weight cut-off, Amicon Ultra, Merck Millipore). Next, the protein was loaded onto an anion exchange Q Sepharose column (HiTrap™ Q HP, GE Healthcare) and purified using an AKTA or AKTAexpress purifier FPLC system (GE healthcare). The enzyme was eluted from the Q-column by running a gradient from 0 to 0.5 M NaCl over 10 column volumes. Fractions containing the enzyme were pooled, concentrated, and exchanged into storage buffer (25 mM tris-HCl, 25 mM NaCl, pH 7.5) as before. Subsequently, the concentrated protein was aliquoted, flash-frozen on powdered dry ice, and stored at –80 ºC. Protein concentrations were determined via Bradford assay with a bovine serum albumin standard curve.

Proteins used for other purposes were eluted from the Ni-NTA column as described above, pooled, concentrated, and subjected to three exchanges of phosphate buffer (0.1 M KPi, pH 8.0) using centrifugal filters (10 kDa molecular weight cut-off, Amicon Ultra, Merck Millipore) to remove excess salt and imidazole. Concentrated proteins were aliquoted, flash-frozen on powdered dry ice, and stored at –80 or –20 ºC.

Amination bioconversions using purified protein. Aliquots of phosphate buffer (260 μL 0.1 M KPi, pH 8.0) and NADPH (40 μL, 100 mM), or multiples thereof, were combined in a 6-mL crimp vial and degassed by sparging with argon for at least 30 minutes. Separately, a glucose solution (250 mM in 0.1 M KPi, pH 8.0) was also degassed in the same manner. Crimp vials (2 mL) were each charged with the oxygen depletion system (20 μL of a stock solution containing 14,000 U/mL catalase and 1,000 U/mL glucose oxidase in 0.1 M KPi, pH 8.0). After degassing was complete, all solutions, 2-mL crimp vials, and purified protein (100 μM in 0.1 M KPi, pH 8.0), kept on ice, were brought into the anaerobic chamber. Glucose solution (40 μL), NADPH

solution (300 μL), and purified protein (20 μL of 100 μM stock solution) were added to each 2-mL vial. Reaction vials were then charged with alkane (10 μL, 200 mM in DMSO) and tosyl azide (10 μL, 200 mM in DMSO). Final concentrations were typically 5 mM alkane, 5 mM tosyl azide, 10 mM NADPH, 25 mM glucose, and 5 μM P411; final reaction volume was 400 μL. The vials were sealed, removed from the anaerobic chamber, and shaken at room temperature and 40 rpm for 16–20 h. The reactions were quenched by addition of acetonitrile (400 μL) and internal standard (10 μL of a DMSO stock). This mixture was then transferred to a microcentrifuge tube and centrifuged at 20,000 x g for 10 minutes. The supernatant was transferred to a vial and analyzed by HPLC. Sodium dithionite (5 mM) was used as the reductant instead of NADPH for reactions with hemin and myoglobin.

Supplementary Table 1. C–H amination of 4-ethylanisole with variants of cytochrome $P450_{BM3}$.[a]

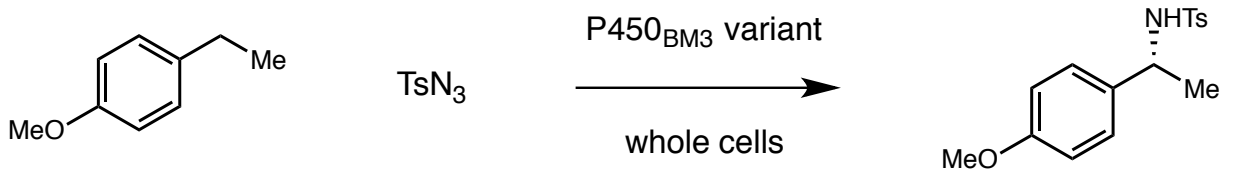

Variant	Mutations relative to wild-type $P450_{BM3}$	Yield
pET22b(+) vector	N/A	N.D.
$P450_{BM3}$	None	N.D.
$P411_{BM3}$	C400S	N.D.
$P411_{BM3}$ T268A	T268A, C400S	N.D.
$P411_{BM3}$-CIS T438S ("P")	V78A, F87V, P142S, T175I, A184V, S226R, H236Q, E252G, T268A, A290V, L353V, I366V, C400S, T438S, E442K	N.D.
$P411_{BM3}$-CIS T438S A268T	V78A, F87V, P142S, T175I, A184V, S226R, H236Q, E252G, A290V, L353V, I366V, C400S, T438S, E442K	N.D.
$P411_{BM3}$-H2-5-F10	L75A, V78A, F87V, P142S, T175I, A184V, S226R, H236Q, E252G, I263A, T268A, A290V, L353V, I366V, C400S, L437A, E442K	N.D.
$P411_{BM3}$-H2-A-10	L75A, V78A, F87V, P142S, T175I, L181A, A184V, S226R, H236Q, E252G, T268A, A290V, L353V, I366V, C400S, E442K	N.D.
$P411_{BM3}$-H2-4-D4	L75A, V78A, F87V, P142S, T175I, M177A, L181A, A184V, S226R, H236Q, E252G, T268A, A290V, L353V, I366V,	N.D.

	C400S, L437A, E442K	
$P411_{BM3}$ T268A F87A[b]	F87A, T268A, C400S	N.D.
P-I263F[b]	V78A, F87V, P142S, T175I, A184V, S226R, H236Q, E252G, I263F, T268A, A290V, L353V, I366V, C400S, T438S, E442K	<1% yield
P-I263F A268T	P-I263F A268T	N.D.
P-I263F A328V	P-I263F A328V	<1% yield
P-I263F A328V L437V[c]	P-I263F A328V L437V	N.D.
P-I263F V87A	P-I263F V87A	2% yield
P-I263F V87A A328V	P-I263F V87A A328V	2% yield
P-I263F V87A A328V A82L	P-I263F V87A A328V A82L	4% yield
P-5	P-I263F V87A A328V A268G A82I	14% yield
P-4 A82L A78V F263M[d]	P-4 A82L A78V F263M	55% yield, 99% ee
P-4 A82L A78V F263Y[d]	P-4 A82L A78V F263Y	68% yield, 61% ee
P-4 A82L A78V F263L (heme domain only)	P-4 A82L A78V F263L (heme domain only)	<1% yield

[a]Reactions performed in whole cells at OD_{600} = 30 with 5 mM of each substrate; results are the average of duplicate reactions. N.D. = none detected. [b]Variants identified for regioselective intramolecular C–H amination.[6] [c]Variant identified for aziridination of styrenes.[7] [d]Other active variants identified in the course of evolution of cytochrome $P411_{CHA}$.

Supplementary Table 2. C–H amination of 4-ethylanisole performed with hemin or heme-containing proteins.[a]

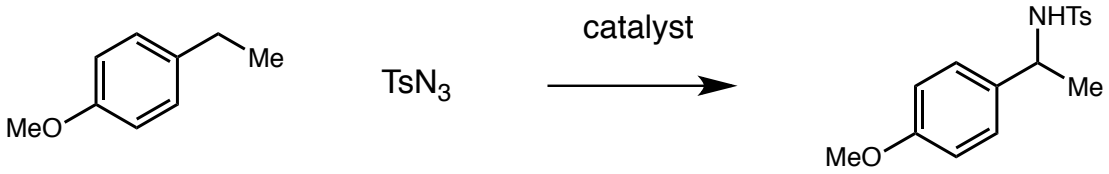

Catalyst	Yield
hemin (25 μM)[b]	N.D.
hemin (25 μM) + imidazole (1 mM)[b]	N.D.
hemin (25 μM) + bovine serum albumin (10 μM)[b]	N.D.
Myoglobin (Mb, equine heart, 10 μM)[b]	N.D.
Mb H64V V68A (sperm whale, 10 μM)[b,c]	N.D.
Rhodothermus marinus cytochrome c[d]	N.D.
Hydrogenobacter thermophilus cytochrome c[d]	N.D.
Rhodopila globiformis cytochrome c[d]	N.D.
Rhodothermus marinus cytochrome c V75T M100D M103E[d,e]	N.D.

[a]Reactions performed with 5 mM 4-ethylanisole and 5 mM tosyl azide; results are the average of duplicate reactions. N.D. = none detected. [b]Performed *in vitro* with 5 mM sodium dithionite. [c]Variant identified for intramolecular C–H amination.[8] [d]Performed in whole cells at OD_{600} = 30. [e]Variant identified for carbene Si–H insertion.[9]

Supplementary Table 3. Mutations present in cytochrome $P450_{BM3}$ variants used in this work.

Variant	Mutations relative to wild-type $P450_{BM3}$
P-4	V78A, F87A, P142S, T175I, A184V, S226R, H236Q, E252G, I263F, T268G, A290V, A328V, L353V, I366V, C400S, T438S, E442K
P-4 A82L	V78A, A82L, F87A, P142S, T175I, A184V, S226R, H236Q, E252G, I263F, T268G, A290V, A328V, L353V, I366V, C400S, T438S, E442K
P-4 A82L A78V	A82L, F87A, P142S, T175I, A184V, S226R, H236Q, E252G, I263F, T268G, A290V, A328V, L353V, I366V, C400S, T438S, E442K
P-4 A82L A78V F263L	A82L, F87A, P142S, T175I, A184V, S226R, H236Q, E252G, I263L, T268G, A290V, A328V, L353V, I366V, C400S, T438S, E442K
P-4 A82L A78V F263L E267D ($P411_{CHA}$)	A82L, F87A, P142S, T175I, A184V, S226R, H236Q, E252G, I263L, E267D, T268G, A290V, A328V, L353V, I366V, C400S, T438S, E442K

Supplementary Table 4. Summary of directed evolution for intermolecular C–H amination.[a]

Generation	Parent enzyme	Site-saturation libraries evaluated	Screening substrate	Mutation identified
1	P-4 A82L	A78X, L181X, F263X, T327X	4-ethylanisole	A78V
2	P-4 A82L A78V	F263X, T327X	4-ethylanisole	F263L
3*a*	P-4 A82L A78V F263L	A74X, A264X, F393X, G402X	4-ethylanisole	none
3*b*	P-4 A82L A78V F263L	R47X, S142X, V184X, G252X, E267X	4-ethyltoluene	E267D
4	P-4 A82L A78V F263L E267D ($P411_{CHA}$)	R47X, Y51X	4-ethyltoluene	none

[a]Some residues were saturated more than once, in different parent variants.

A74, L181, F263, A264, E267, T327: Distal face of heme, active site residues

F393, G402: Axial face of heme

A78, S142, V184, G252: Already mutated in P-4 relative to wild type $P450_{BM3}$

R47, Y51: Polar residues that interact with the carboxylate of the native fatty acid substrates

Supplementary Table 5. Intermolecular C–H amination data presented in Figure 3.

Variant	Substrate	[P411]	Yield	ee	TON
P-4	4-ethylanisole	1.8 μM	11 ± 1%	14% (*S*)	310
P-4 A82L	4-ethylanisole	2.4 μM	51 ± 3%	77% (*R*)	1000
P-4 A82L A78V	4-ethylanisole	2.7 μM	66 ± 2%	80% (*R*)	1200
P-4 A82L A78V F263L	4-ethylanisole	N.A.[a]	66 ± 2%	>99% (*R*)	N.A.[a]
$P411_{CHA}$	4-ethylanisole	3.2 μM	66 ± 3%	>99% (*R*)	1000
P-4	4-ethyltoluene	1.8 μM	2.0 ± 0.3%	N.A.	58
P-4 A82L	4-ethyltoluene	2.4 μM	11 ± 1%	98% ee (*R*)	220
P-4 A82L A78V	4-ethyltoluene	2.7 μM	29 ± 1%	>99% ee (*R*)	530
P-4 A82L A78V F263L	4-ethyltoluene	N.A.[a]	32 ± 1%	>99% ee (*R*)	N.A.[a]
$P411_{CHA}$	4-ethyltoluene	3.2 μM	34 ± 3%	>99% ee (*R*)	530
P-4	ethylbenzene	1.8 μM	0.50 ± 0.01%	N.A.	15
P-4 A82L	ethylbenzene	2.4 μM	2.2 ± 0.1%	N.A.	46
P-4 A82L A78V	ethylbenzene	2.7 μM	6.5 ± 0.4%	92% ee (*R*)	120
P-4 A82L A78V F263L	ethylbenzene	N.A.[a]	6.7 ± 0.4%	>99% ee (*R*)	N.A.[a]
$P411_{CHA}$	ethylbenzene	3.2 μM	15 ± 1%	>99% ee (*R*)	240

[a]Protein concentration could not be accurately determined; variant is poorly behaved in carbon monoxide-binding assay.

Supplementary Table 6. Activity of P411 variants toward C–H amination of indan, tetralin, 1-bromo-4-ethylbenzene, and 4-propylanisole. Reactions were performed as in Table 2 (2.5 mM alkane, 5.0 mM tosyl azide).

Substrate	**Product**	**P-4 A82L A78V F263L**	**P411$_{CHA}$**
indan	*N*-tosyl-1-aminoindane	72% yield, 90% ee	80% yield, 96% ee
tetralin	*N*-tosyl-1-aminotetralin	49% yield, 81% ee	76% yield, 95% ee
1-bromo-4-ethylbenzene	*N*-tosyl-1-(*p*-bromophenyl)ethylamine	13% yield, >99% ee	19% yield, >99% ee
4-propylanisole	*N*-tosyl-1-(*p*-methoxyphenyl)propylamine	15% yield, >99% ee	16% yield, >99% ee

Supplementary Table 7. C–H amination reactions performed under aerobic conditions.[a]

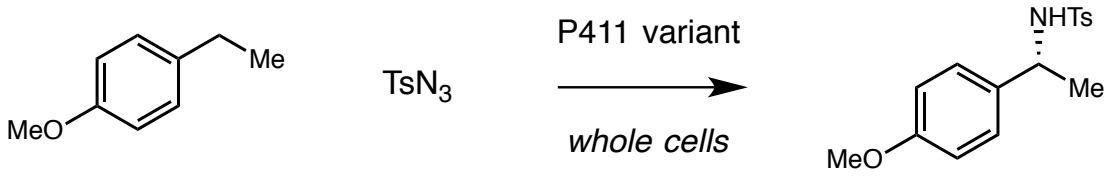

Variant	Conditions	Yield
P-4 A82L A78V	anaerobic, full system	66%
P-4 A82L A78V	aerobic, full system	13%
P-4 A82L A78V	aerobic, no glucose oxidase/catalase	7.5%
P-4 A82L A78V F263L	anaerobic, full system	66%
P-4 A82L A78V F263L	aerobic, full system	20%
P-4 A82L A78V F263L	aerobic, no glucose oxidase/catalase	7.6%
$P411_{CHA}$	anaerobic, full system	66%
$P411_{CHA}$	aerobic, full system	15%
$P411_{CHA}$	aerobic, no glucose oxidase/catalase	9.5%

[a]Reactions performed as in Figure 3 (5 mM 4-ethylanisole, 5 mM tosyl azide). For reactions without the glucose oxidase/catalase mixture, 20 μL of M9-N media was added instead.

Supplementary Table 8. C–H amination of 4-ethylanisole performed with purified P411 variants.[a]

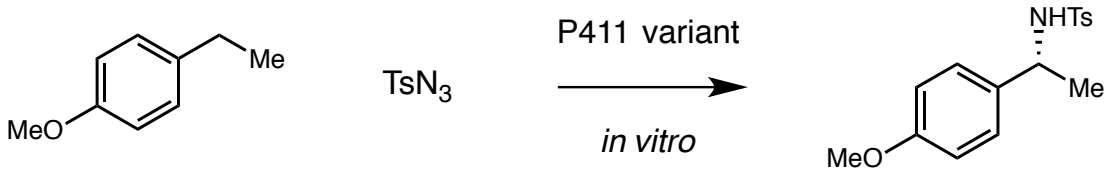

Catalyst	Yield, turnovers, ee
P-4 (5 μM)	2.2% yield, 22 TON, 4% ee *(S)*
P-4 A82L (5 μM)	9.7% yield, 97 TON, 80% ee (*R*)
P-4 A82L A78V F263L (5 μM)	19% yield, 190 TON, >99% ee (*R*)
$P411_{CHA}$ (5 μM)	15% yield, 150 TON, >99% ee (*R*)
$P411_{CHA}$ (20 μM)	47% yield, 120 TON, >99% ee (*R*)
P-4 A82L A78V F263L (heme domain only, 10 μM)[b]	1.4% yield, 7 TON

[a]Reactions performed with 10 mM NADPH, 5 mM 4-ethylanisole, and 5 mM tosyl azide; results are the average of duplicate reactions. [b]Performed with 5 mM sodium dithionite instead of NADPH.

Supplementary Table 9. Reaction mass balances; representative reactions showing amount of *p*-toluenesulfonamide ($TsNH_2$, **5**) formed. Reactions are those in Table 2 (performed with 2.5 mM alkane, 5 mM tosyl azide).

Table 2 entry	Substrate	C–H amination product	*p*-toluene-sulfonamide	Total of nitrogen-containing products
1	4-ethylanisole	2.14 mM	2.74 mM	4.88 mM
2	4-ethyltoluene	1.33 mM	3.51 mM	4.84 mM
5	ethylbenzene	0.39 mM	4.63 mM	5.01 mM

Supplementary Table 10. Enantioselective C–H amination of isochroman with cytochrome $P411_{CHA}$ followed by post-reaction racemization.[a]

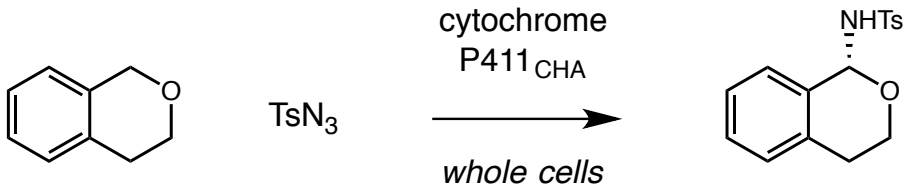

Entry	Conditions	ee
1	1 hour reaction time	65%
2	2 hour reaction time	65%
3	4 hour reaction time	65%
4	6 hour reaction time	65%
5	20 hour reaction time	65%
6	20 hour reaction time, followed by treatment with silica	racemic

[a]Reactions performed as in Table 2, using whole *E. coli* cells overexpressing $P411_{CHA}$ at OD_{600} = 30 (~3 μM enzyme), with 2.5 mM alkane and 5 mM tosyl azide. Identical small scale reactions (400 μL) were set up in parallel. After the indicated time, crude reaction mixtures were extracted with 1:1 cyclohexane:ethyl acetate, concentrated to dryness, and redissolved in 50% isopropanol in cyclohexane. Silica treatment was performed by allowing the crude reaction mixture (in cyclohexane/ethyl acetate) to rest on a silica pipette column (approx. 1 hour) followed by elution with ethyl acetate. Samples were analyzed by SFC chromatography using Chiralpak AS column (35% isopropanol).

Representative traces. Racemic standard, *N*-tosyl-isochroman-1-amine:

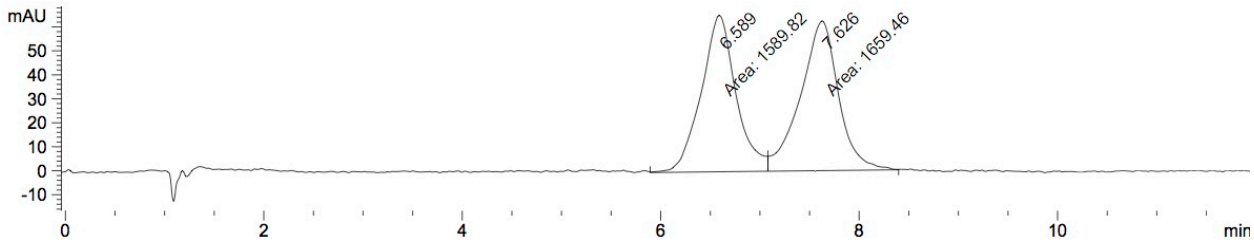

Supplementary Table 10, Entry 5, with P411$_{CHA}$ (65% ee):

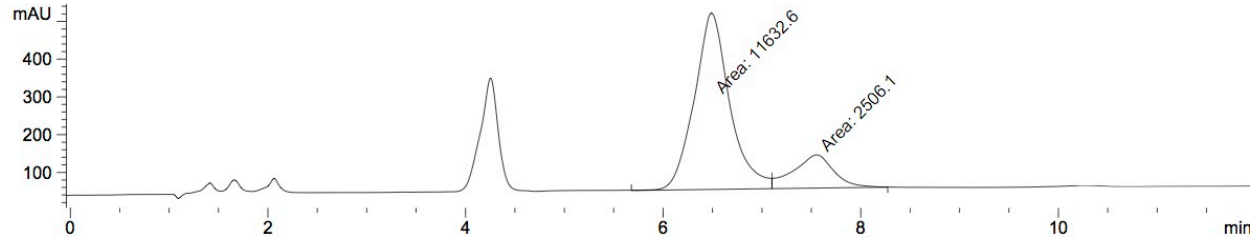

Supplementary Table 10, Entry 6, with P411$_{CHA}$ post silica treatment (racemic):

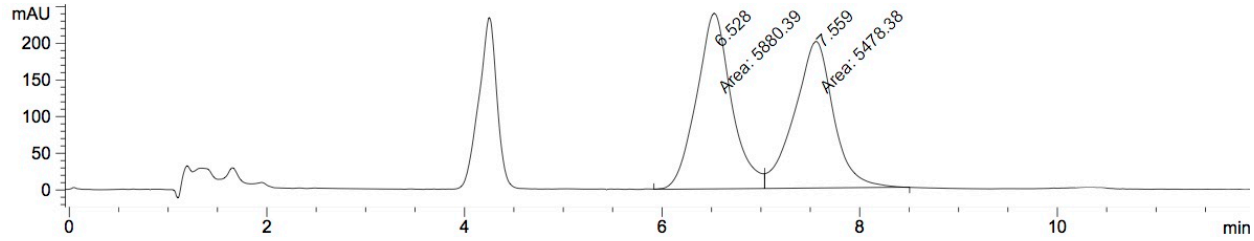

Supplementary Table 11. Thermostabilities of cytochrome P411 variants in the evolutionary lineage. The T_{50} is the temperature at which half of the enzyme population has unfolded after a 10-minute incubation.

P411 Variant	Number of mutations from wild-type	T_{50} (°C)
P-4	17	58.3 ± 0.6
P-4 A82L	18	64.1 ± 0.6
P-4 A82L A78V F263L	17	62.9 ± 0.2
$P411_{CHA}$	18	61.2 ± 0.2

P-4:

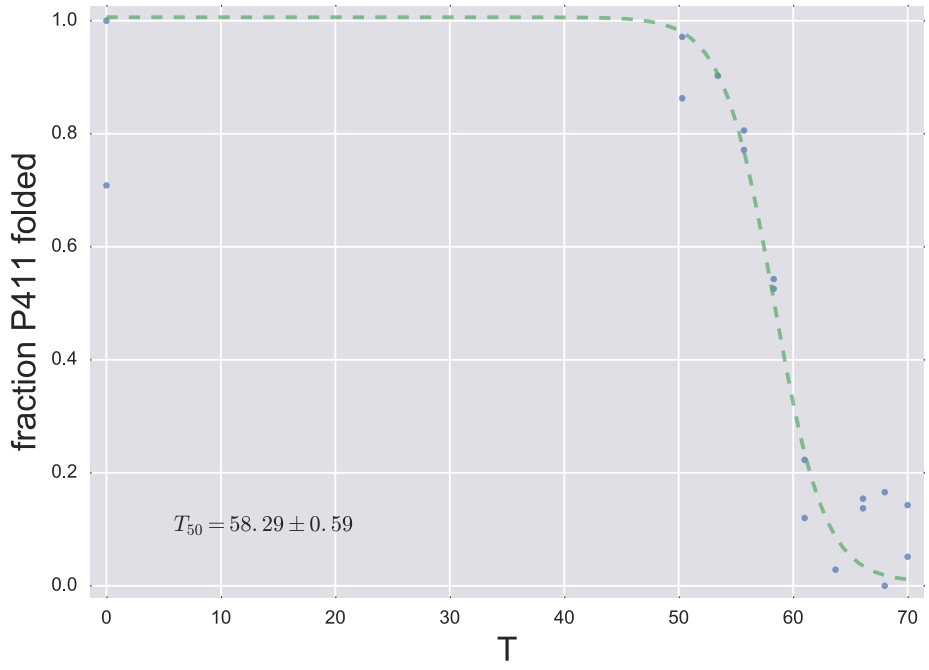

P-4 A82L:

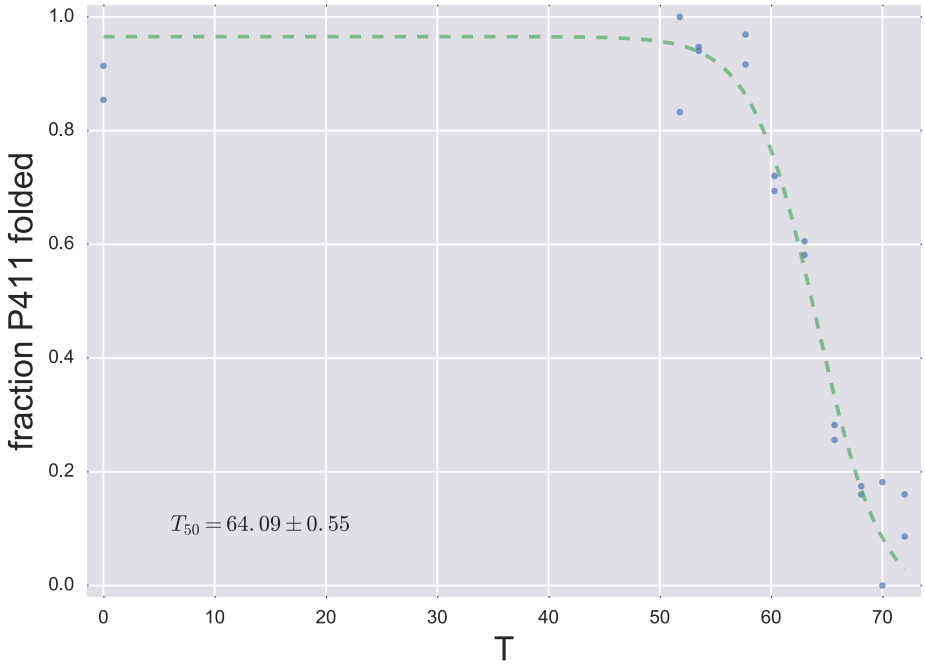

P-4 A82L A78V F263L:

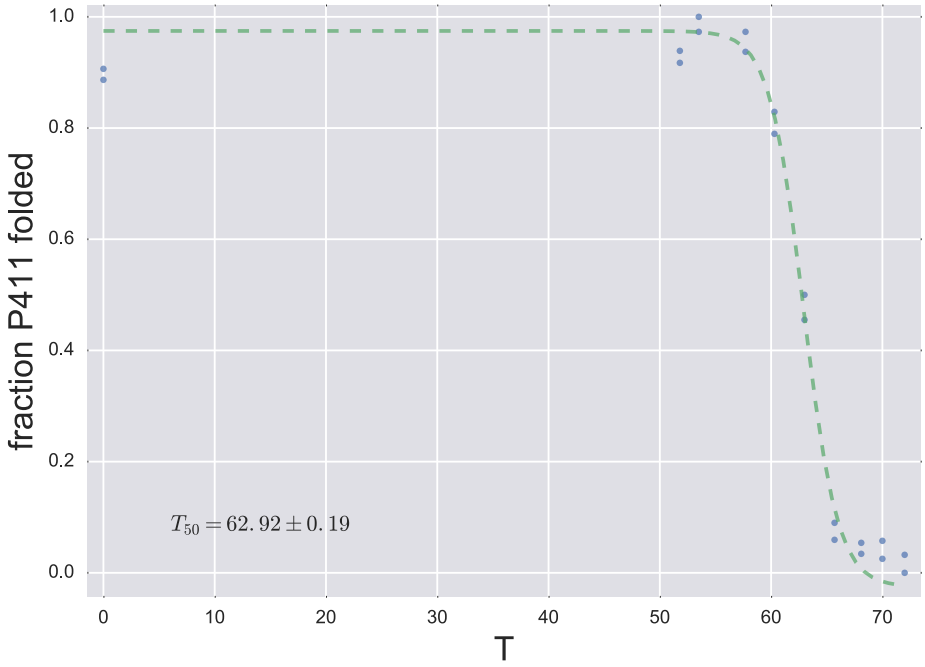

$P411_{CHA}$:

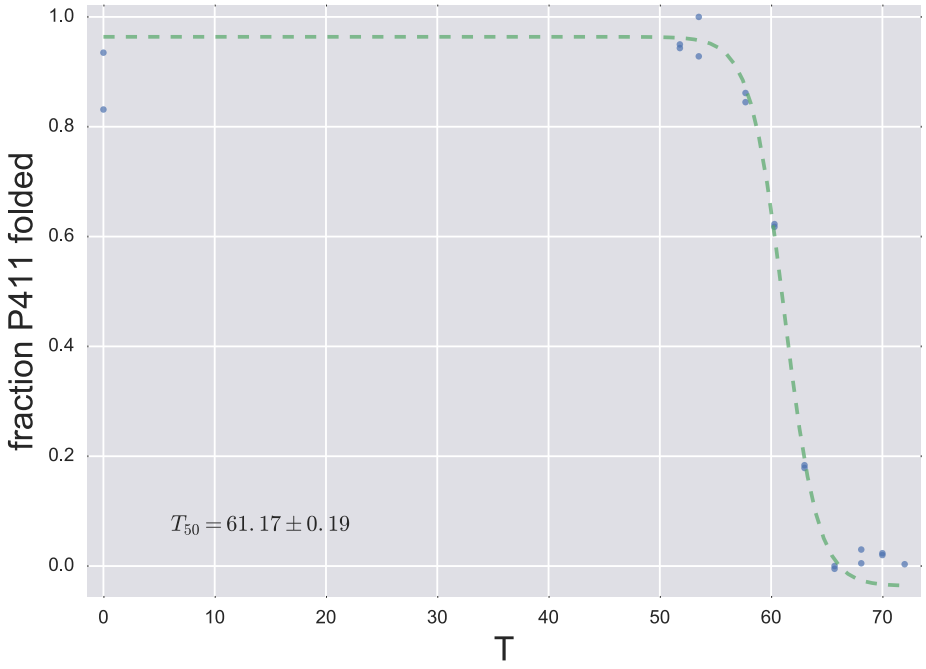
fraction P411 folded
T
$T_{50} = 61.17 \pm 0.19$
1.0
0.8
0.6
0.4
0.2
0.0
0
10
20
30
40
50
60
70

Supplementary Figure 1. Unreactive substrates. Substrates for which C–H amination activity was not detected (or <1% yield) using cytochrome $P411_{CHA}$.

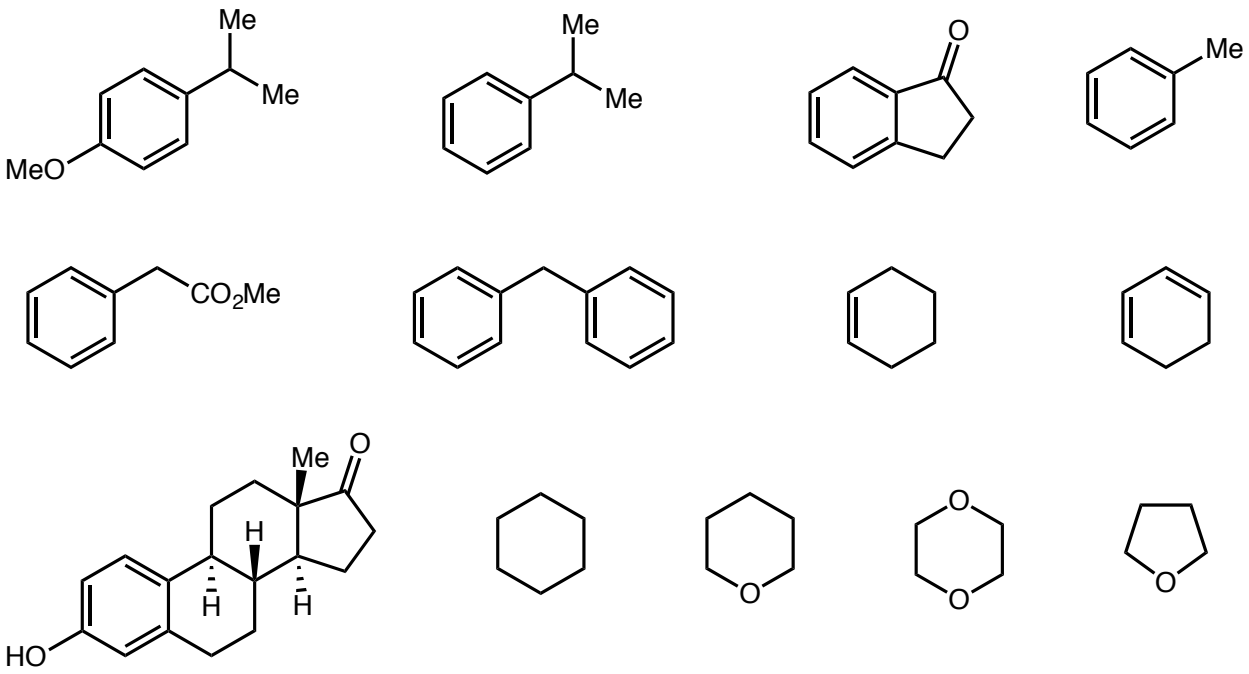

Characterization of reaction products. Authentic standards corresponding to enzymatic reaction products were prepared by tosylation of the corresponding benzylic amine or by racemic C–H amination.[10] Most products are known compounds, and their spectral data are in agreement with reported values.[10–15] New compounds were fully characterized.

***N*-Tosyl-1-(*p*-methoxyphenyl)ethylamine (Table 2, entry 1):** ^{1}H NMR (300 MHz, $CDCl_3$) δ 7.62 (d, *J* = 8.3 Hz, 2H), 7.19 (d, *J* = 8.7 Hz, 2H), 7.05–7.15 (m, 2H), 6.75–6.67 (m, 2H), 4.97 (d, *J* = 6.8 Hz, 1H), 4.40 (p, *J* = 6.8 Hz, 1H), 3.75 (s, 3H), 2.39 (s, 3H), 1.40 (d, *J* = 6.8 Hz, 3H).

***N*-Tosyl-1-(*p*-tolyl)ethylamine (Table 2, entry 2):** ^{1}H NMR (300 MHz, $CDCl_3$) δ 7.62 (d, *J* = 8.3 Hz, 2H), 7.20 (d, *J* = 7.9 Hz, 2H), 7.05–6.95 (m, 4H), 4.65 (d, *J* = 6.8 Hz, 1H), 4.41 (p, *J* = 6.8 Hz, 1H), 2.40 (s, 3H), 2.28 (s, 3H), 1.41 (d, *J* = 6.8 Hz, 3H).

***N*-Tosyl-1-(*m*-tolyl)ethylamine (Table 2, entry 3):** ^{1}H NMR (300 MHz, $CDCl_3$) δ 7.60 (d, *J* = 8.3 Hz, 2H), 7.18 (d, *J* = 7.9 Hz, 2H), 7.09 (t, *J* = 7.6 Hz, 1H), 7.02–6.96 (m, 1H), 6.93–6.87 (m, 1H), 6.83–6.80 (m, 1H), 4.68 (d, *J* = 6.9 Hz, 1H), 4.42 (p, *J* = 6.8 Hz, 1H), 2.39 (s, 3H), 2.22 (s, 3H), 1.42 (d, *J* = 6.8 Hz, 3H).

***N*-Tosyl-1-(*o*-tolyl)ethylamine (Table 2, entry 4):** ^{1}H NMR (300 MHz, $CDCl_3$) δ 7.58 (d, *J* = 8.3 Hz, 2H), 7.18–6.98 (m, 6H), 4.78–4.66 (m, 2H), 2.37 (s, 3H), 2.19 (s, 3H), 1.39 (d, *J* = 6.6 Hz, 3H). Reactions with $P411_{CHA}$ produce a trace amount of the regioisomer *N*-tosyl-(2-ethylphenyl)methanamine (>20:1 r.r. in favor of the secondary benzylic amination product): ^{1}H NMR (400 MHz, $CDCl_3$) δ 7.78 (d, *J* = 8.3 Hz, 2H), 7.33 (d, *J* = 7.9 Hz, 2H), 7.26–7.20 (m, 1H), 7.17 (d, *J* = 7.4 Hz, 1H), 7.13–7.09 (m, 2H), 4.38 (t, *J* = 5.8 Hz, 1H), 4.11 (d, *J* = 5.9 Hz, 2H), 2.57 (q, *J* = 7.6 Hz, 2H), 2.45 (s, 3H), 1.15 (t, *J* = 7.6 Hz, 3H); ^{13}C NMR (100 MHz, $CDCl_3$) δ 143.7, 142.9, 136.6, 133.3, 130.0, 129.3, 129.0, 128.6, 127.4, 126.3, 45.0, 25.2, 21.7, 15.3; IR (film) 3278, 2966, 1451, 1421, 1325, 1158, 1093, 1048, 814, 662 cm^{-1}; HRMS (FAB+) exact mass calculated for $C_{16}H_{20}NO_2S^+$ requires *m/z* 290.1215, found 290.1221.

***N*-Tosyl-1-phenylethylamine (Table 2, entry 5):** ^{1}H NMR (300 MHz, $CDCl_3$) δ 7.62 (d, *J* = 8.3 Hz, 2H), 7.24–7.14 (m, 5H), 7.13–7.06 (m, 2H), 4.94 (d, *J* = 7.0 Hz, 1H), 4.46 (p, *J* = 6.9 Hz, 1H), 2.38 (s, 3H), 1.42 (d, *J* = 6.9 Hz, 3H).

***N*-Tosyl-1-(*p*-bromophenyl)ethylamine (Table 2, entry 6):** ^{1}H NMR (400 MHz, $CDCl_3$) δ 7.57 (d, *J* = 8.3 Hz, 2H), 7.30 (d, *J* = 8.5 Hz, 2H), 7.18 (d, *J* = 7.8 Hz, 2H), 6.97 (d, *J* = 8.3 Hz, 2H), 4.78 (d, *J* = 6.8 Hz, 1H), 4.43 (p, *J* = 6.9 Hz, 1H), 2.40 (s, 3H), 1.39 (d, *J* = 6.9 Hz, 3H).

***N*-Tosyl-1-(*p*-chlorophenyl)ethylamine (Table 2, entry 7):** ^{1}H NMR (300 MHz, $CDCl_3$) δ 7.57 (d, *J* = 8.3 Hz, 2H), 7.22–7.12 (m, 4H), 7.05–7.00 (m, 2H), 4.70 (d, *J* = 6.7 Hz, 1H), 4.45 (p, *J* = 6.9 Hz, 1H), 2.40 (s, 3H), 1.39 (d, *J* = 6.8 Hz, 3H).

***N*-Tosyl-1-(*p*-fluorophenyl)ethylamine (Table 2, entry 8):** ^{1}H NMR (300 MHz, $CDCl_3$) δ 7.59 (d, *J* = 8.3 Hz, 2H), 7.24–7.14 (m, 2H), 7.13–7.03 (m, 2H), 6.94–6.80 (m, 2H), 4.77 (d, *J* = 6.7 Hz, 1H), 4.46 (p, *J* = 6.8 Hz, 1H), 2.39 (s, 3H), 1.40 (d, *J* = 6.9 Hz, 3H).

***N*-Tosyl-1-aminoindane (Table 2, entry 9):** ^{1}H NMR (400 MHz, $CDCl_3$) δ 7.84 (d, *J* = 8.3 Hz, 2H), 7.38–7.32 (m, 2H), 7.25–7.12 (m, 3H), 7.08 (d, *J* = 7.4 Hz, 1H), 4.84 (q, *J* = 7.8 Hz, 1H), 4.60 (d, *J* = 9.0 Hz, 1H), 2.90 (ddd, *J* = 16.0, 8.7, 3.7 Hz, 1H), 2.75 (dt, *J* = 16.3, 8.2 Hz, 1H), 2.46 (s, 3H), 2.40–2.29 (m, 1H), 1.82–1.69 (m, 1H).

***N*-Tosyl-1-aminotetralin (Table 2, entry 10):** ^{1}H NMR (300 MHz, $CDCl_3$) δ 7.83 (d, *J* = 8.3 Hz, 2H), 7.39–7.31 (m, 2H), 7.20–6.90 (m, 4H), 4.59 (d, *J* = 7.7 Hz, 1H), 4.45 (dt, *J* = 7.9, 4.6 Hz, 1H), 2.85–2.57 (m, 2H), 2.47 (s, 3H), 1.95–1.62 (m, 4H).

***N*-Tosyl-3-amino-2,3-dihydrobenzofuran (Table 2, entry 11):** ^{1}H NMR (400 MHz, $CDCl_3$) δ 7.81 (d, *J* = 8.3 Hz, 2H), 7.37 (d, *J* = 7.9 Hz, 2H), 7.23–7.17 (m, 1H), 6.94–6.88 (m, 1H), 6.86–6.78 (m, 2H), 5.05 (ddd, *J* = 8.1, 8.1, 4.1 Hz, 1H), 4.77 (d, *J* = 8.5 Hz, 1H), 4.49 (dd, *J* = 10.3, 7.9 Hz, 1H), 4.28 (dd, *J* = 10.3, 4.1 Hz, 1H), 2.48 (s, 3H); ^{13}C NMR (100 MHz, $CDCl_3$) δ 160.0, 144.1, 137.8, 130.9, 130.2, 127.3, 125.3, 125.0, 121.4, 110.7, 77.4, 55.6, 21.8; IR (film)

3284, 2921, 1598, 1482, 1330, 1155, 1082, 970, 750, 667 cm^{-1}; HRMS (FAB+) exact mass calculated for $C_{15}H_{16}NO_3S^+$ requires *m/z* 290.0851, found 290.0855.

***N*-Tosyl-1-(2-naphthyl)ethylamine (Table 2, entry 12):** ^{1}H NMR (400 MHz, $CDCl_3$) δ 7.78–7.72 (m, 1H), 7.66 (d, *J* = 8.8 Hz, 2H), 7.57 (d, *J* = 8.3 Hz, 2H), 7.48–7.41 (m, 3H), 7.20 (dd, J = 8.5, 1.8 Hz, 1H), 7.06–7.01 (m, 2H), 4.90 (d, *J* = 7.0 Hz, 1H), 4.64 (p, *J* = 6.9 Hz, 1H), 2.25 (s, 3H), 1.52 (d, *J* = 6.8 Hz, 3H).

***N*-Tosyl-1-(1-naphthyl)ethylamine (Table 2, entry 13):** ^{1}H NMR (300 MHz, $CDCl_3$) δ 7.92–7.77 (m, 2H), 7.69 (d, *J* = 7.6 Hz, 1H), 7.57 (d, *J* = 8.3 Hz, 2H), 7.50–7.26 (m, 4H), 7.07 (d, *J* = 7.7 Hz, 2H), 5.28 (p, *J* = 6.8 Hz, 1H), 4.94 (d, *J* = 6.7 Hz, 1H), 2.33 (s, 3H), 1.60 (d, *J* = 6.8 Hz, 3H).

***N*-Tosyl-1-(*p*-methoxyphenyl)propylamine (Table 2, entry 14):** ^{1}H NMR (400 MHz, $CDCl_3$) δ 7.54 (d, *J* = 8.3 Hz, 2H), 7.13 (d, *J* = 7.8 Hz, 2H), 6.92 (d, *J* = 8.6 Hz, 2H), 6.68 (d, *J* = 8.7 Hz, 2H), 4.77 (d, *J* = 7.0 Hz, 1H), 4.13 (q, *J* = 7.1 Hz, 1H), 3.75 (s, 3H), 2.37 (s, 3H), 1.88–1.62 (m, 2H), 0.76 (t, *J* = 7.4 Hz, 3H).

***N*-Tosyl-4-methoxybenzylamine (Table 2, entry 15):** ^{1}H NMR (400 MHz, $CDCl_3$) δ 7.76 (d, *J* = 8.3 Hz, 2H), 7.34–7.29 (m, 2H), 7.11 (d, *J* = 8.9 Hz, 2H), 6.80 (d, J = 8.8 Hz, 2H), 4.52 (t, *J* = 6.1 Hz, 1H), 4.05 (d, *J* = 6.1 Hz, 2H), 3.78 (s, 3H), 2.44 (s, 3H).

***N*-Tosyl-1,3-dihydroisobenzofuran-1-amine (Table 2, entry 16):** ^{1}H NMR (400 MHz, $CDCl_3$) δ 7.86 (d, *J* = 8.4 Hz, 2H), 7.38–7.28 (m, 5H), 7.24–7.18 (m, 1H), 6.55 (dd, *J* = 10.2, 2.1 Hz, 1H), 5.21 (d, *J* = 10.2 Hz, 1H), 5.00 (dd, *J* = 12.6, 2.6 Hz, 1H), 4.91 (d, *J* = 12.6 Hz, 1H), 2.45 (s, 3H).

***N*-Tosyl-isochroman-1-amine (Table 2, entry 17):** ^{1}H NMR (300 MHz, $CDCl_3$) δ 7.86 (d, *J* = 8.4 Hz, 2H), 7.35–7.28 (m, 2H), 7.25–7.18 (m, 3H), 7.12–7.05 (m, 1H), 6.11 (d, *J* = 8.6 Hz, 1H),

5.37 (d, *J* = 8.5 Hz, 1H), 3.74–3.58 (m, 2H), 2.85 (ddd, *J* = 16.5, 9.2, 6.0 Hz, 1H), 2.61 (dt, *J* = 16.6, 3.9 Hz, 1H), 2.44 (s, 3H).

HPLC Calibration: Calibration curves with an internal standard were created for quantitative HPLC analysis of reaction products. The identity of the products was additionally confirmed by HPLC co-injections of reaction mixtures with chemically synthesized authentic products, or by NMR analysis of products isolated from reactions performed on preparative scale.

N-Tosyl-1-(*p*-methoxyphenyl)ethylamine (**4**), with 1.25 mM 1,3,5-trimethoxybenzene as internal standard, at 230 nm.

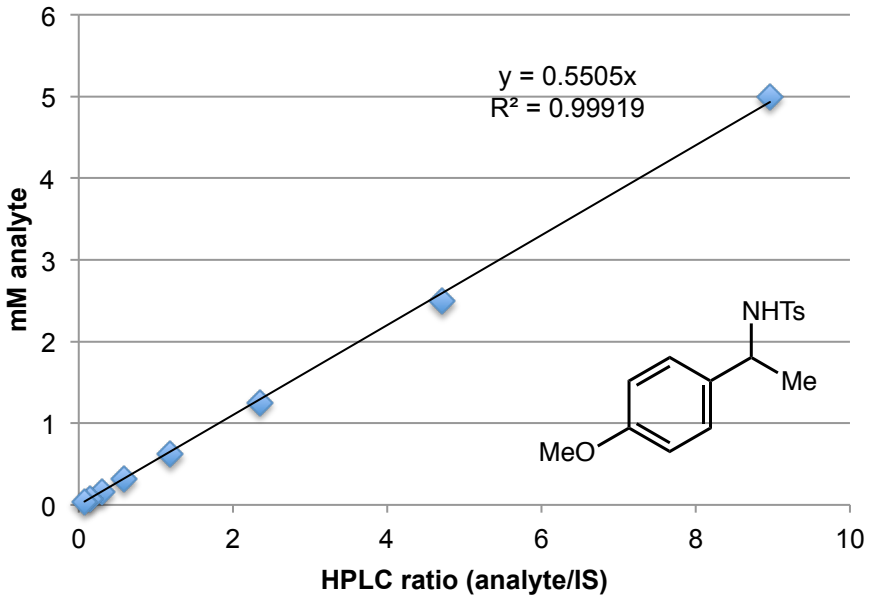

N-Tosyl-1-(*p*-tolyl)ethylamine, with 1.25 mM 1,3,5-trimethoxybenzene as internal standard, at 230 nm.

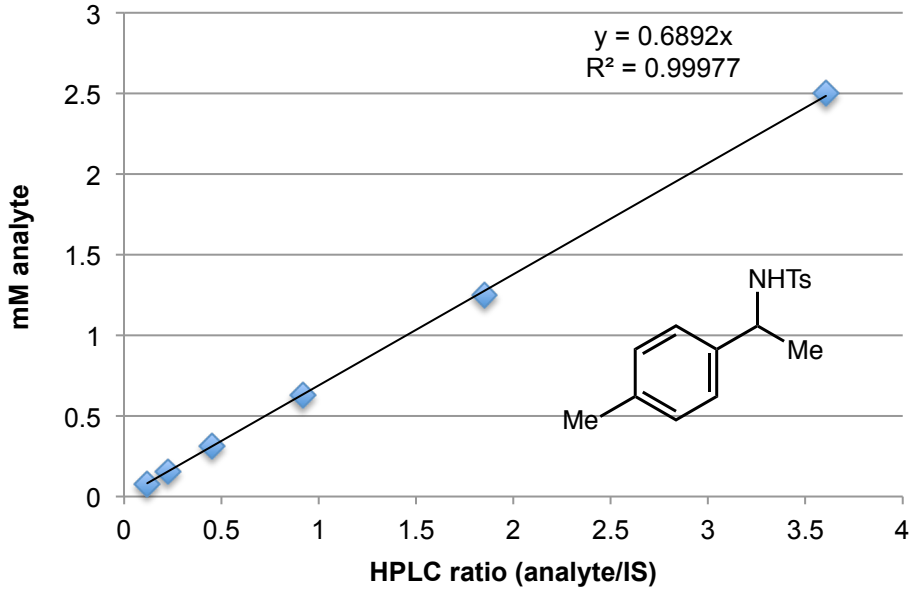

N-Tosyl-1-(*m*-tolyl)ethylamine, with 1.25 mM 1,3,5-trimethoxybenzene as internal standard, at 230 nm.

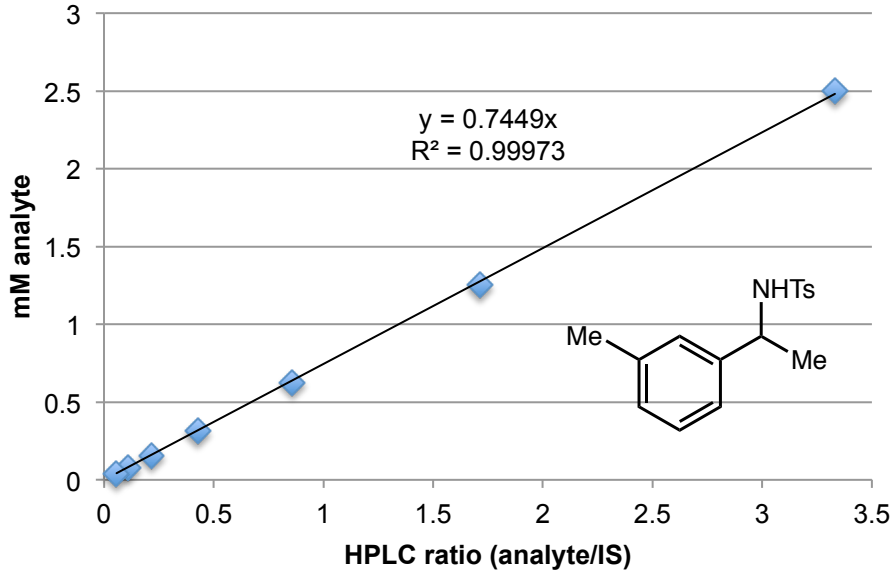

N-Tosyl-1-(*o*-tolyl)ethylamine, with 1.25 mM 1,3,5-trimethoxybenzene as internal standard, at 230 nm.

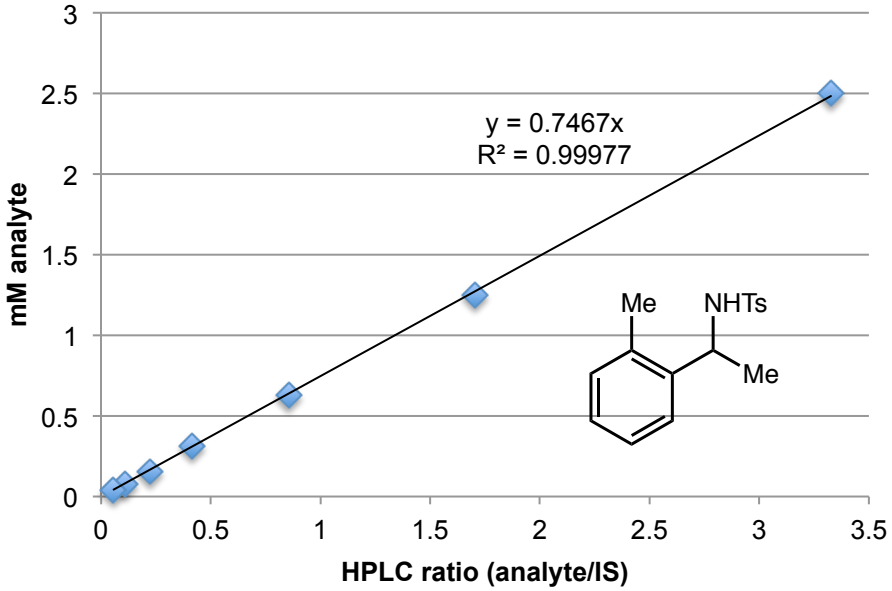

N-Tosyl-1-phenylethylamine, with 1.25 mM 1,3,5-trimethoxybenzene as internal standard, at 230 nm.

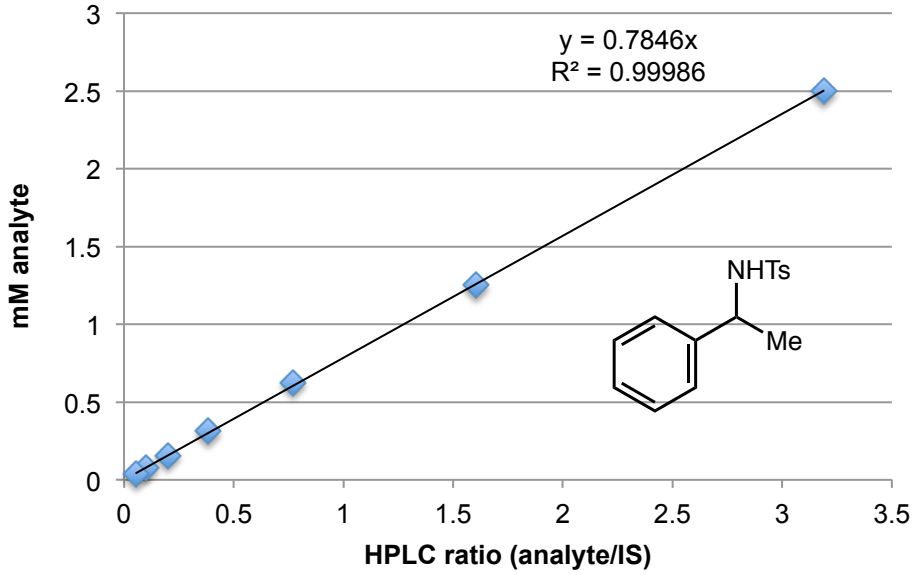

N-Tosyl-1-(*p*-bromophenyl)ethylamine, with 1.25 mM 1,3,5-trimethoxybenzene as internal standard, at 230 nm.

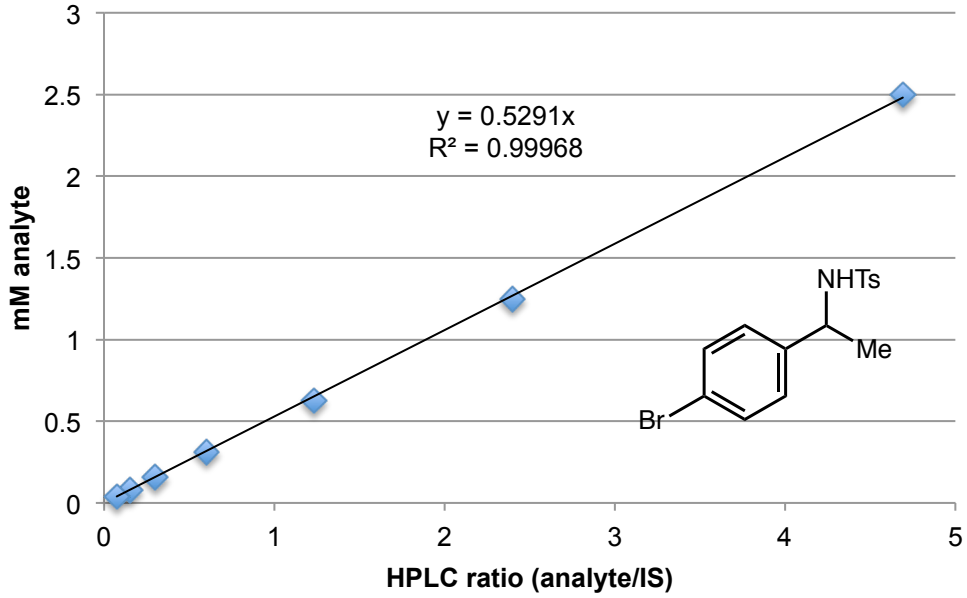

N-Tosyl-1-(*p*-chlorophenyl)ethylamine, with 1.25 mM 1,3,5-trimethoxybenzene as internal standard, at 230 nm.

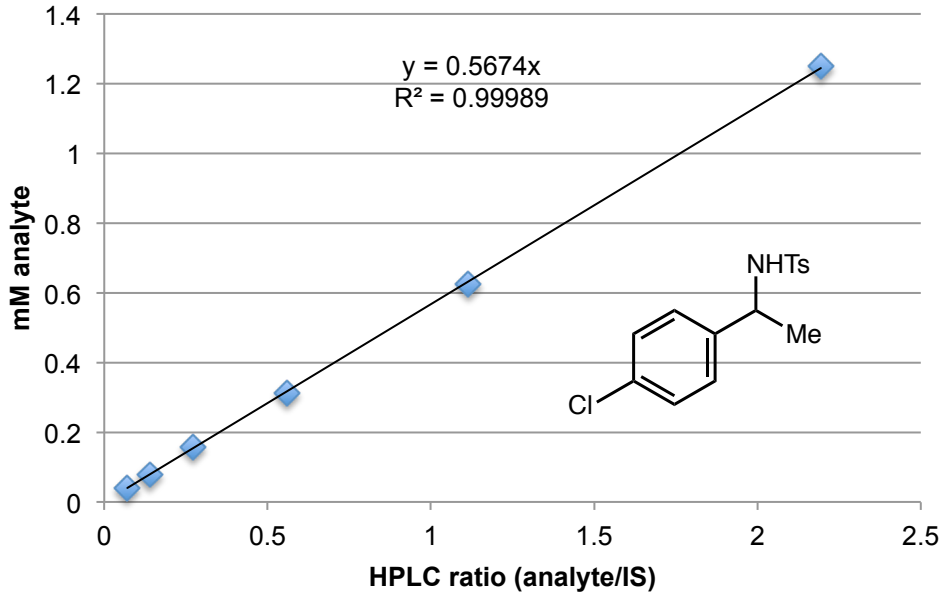

N-Tosyl-1-(*p*-fluorophenyl)ethylamine, with 1.25 mM 1,3,5-trimethoxybenzene as internal standard, at 230 nm.

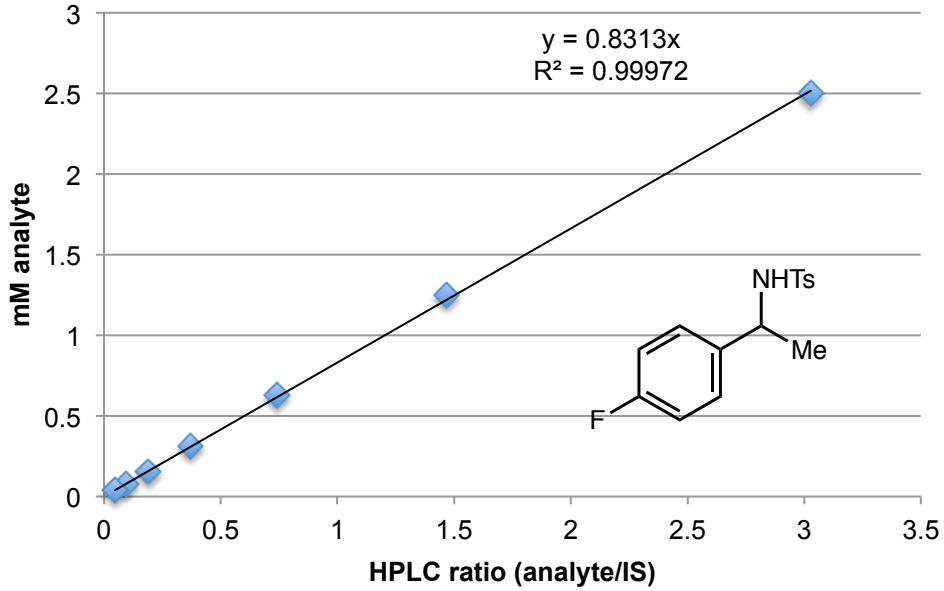

N-Tosyl-1-aminoindane, with 1.25 mM 1,3,5-trimethoxybenzene as internal standard, at 230 nm.

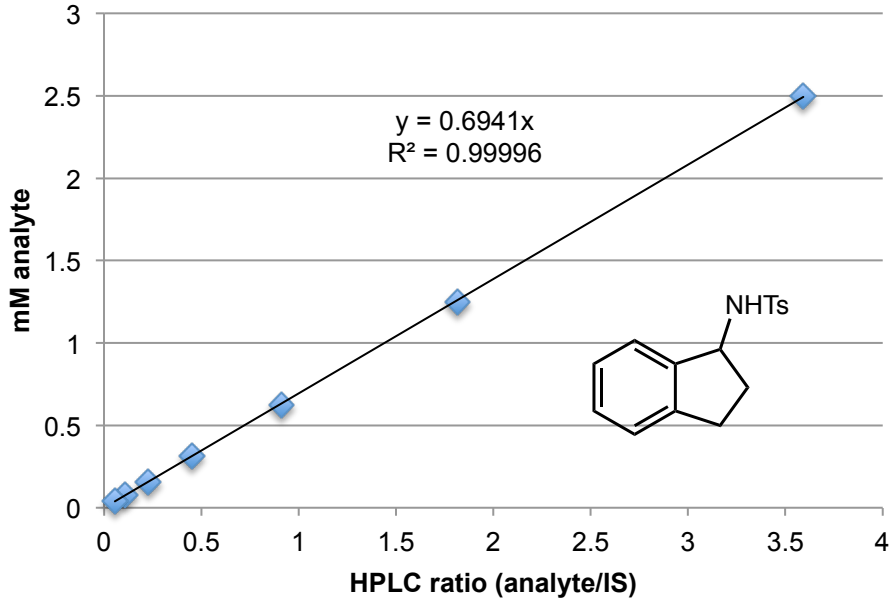

N-Tosyl-1-aminotetralin, with 1.25 mM 1,3,5-trimethoxybenzene as internal standard, at 230 nm.

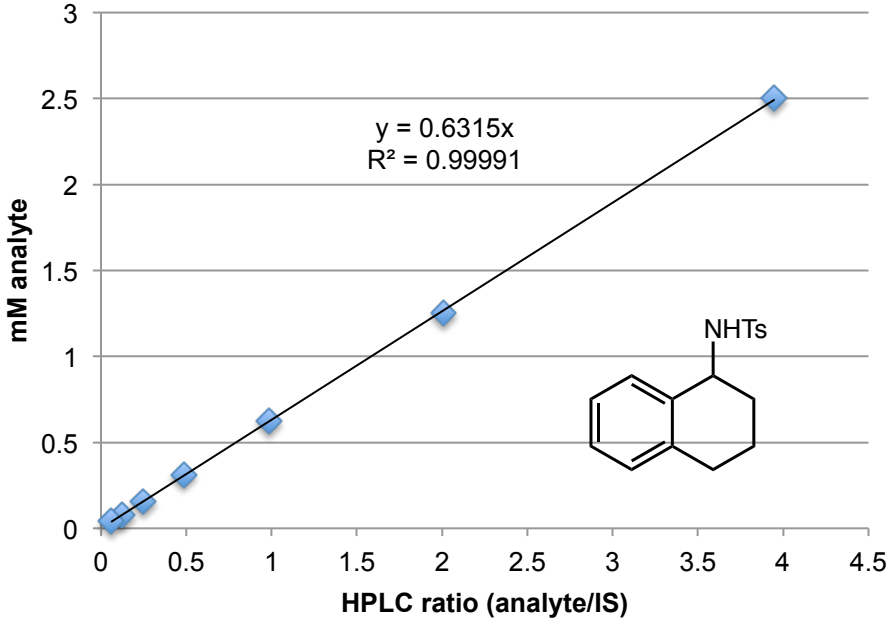

N-Tosyl-1-(2-naphthyl)ethylamine, with 1.25 mM 1,3,5-trimethoxybenzene as internal standard, at 230 nm.

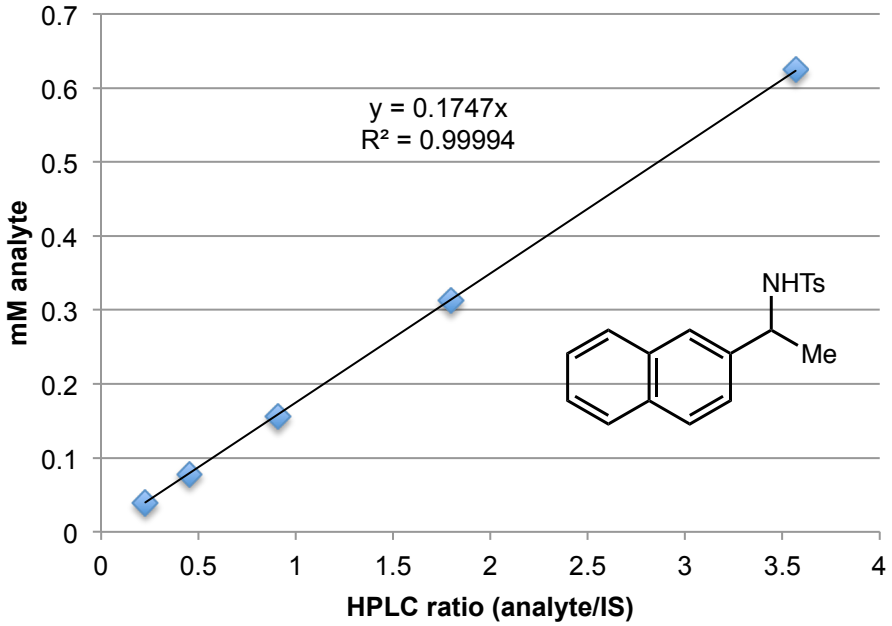

N-Tosyl-1-(1-naphthyl)ethylamine, with 1.25 mM 1,3,5-trimethoxybenzene as internal standard, at 230 nm.

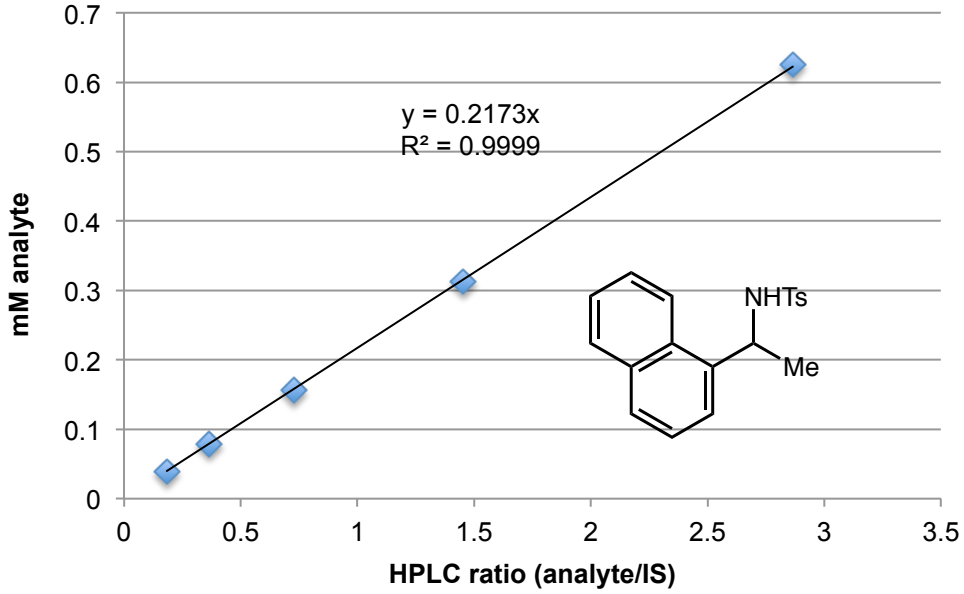

N-Tosyl-1-(*p*-methoxyphenyl)propylamine, with 1.25 mM 1,3,5-trimethoxybenzene as internal standard, at 230 nm.

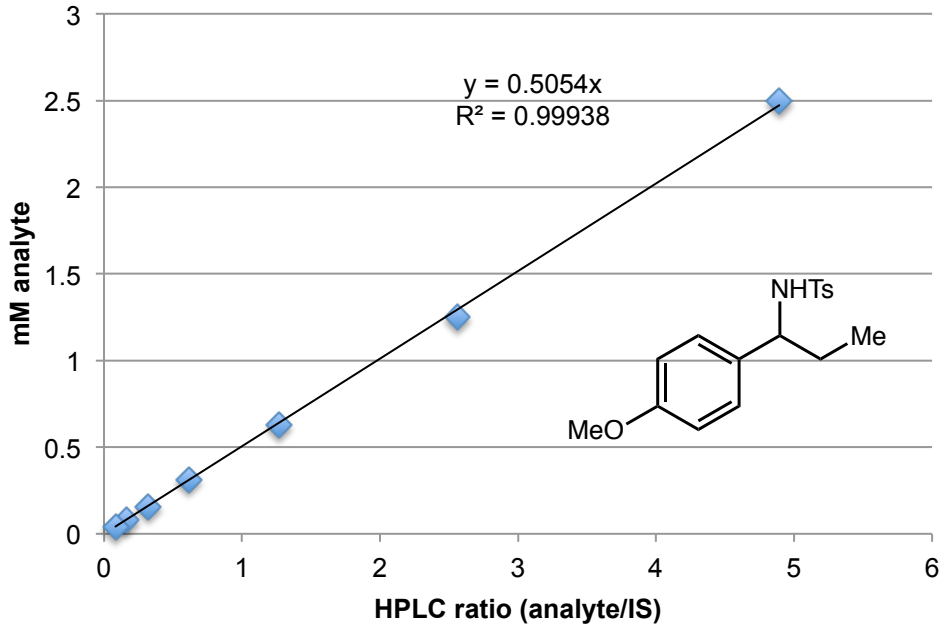

N-Tosyl-4-methoxybenzylamine, with 1.0 mM methyl phenylacetate as internal standard, at 210 nm.

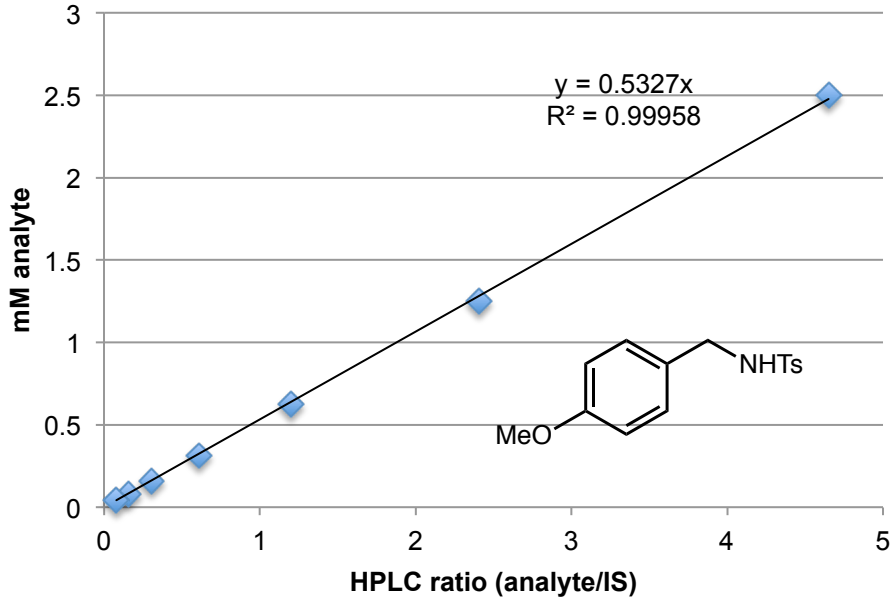

p-Toluenesulfonamide, with 1.25 mM 1,3,5-trimethoxybenzene as internal standard, at 230 nm.

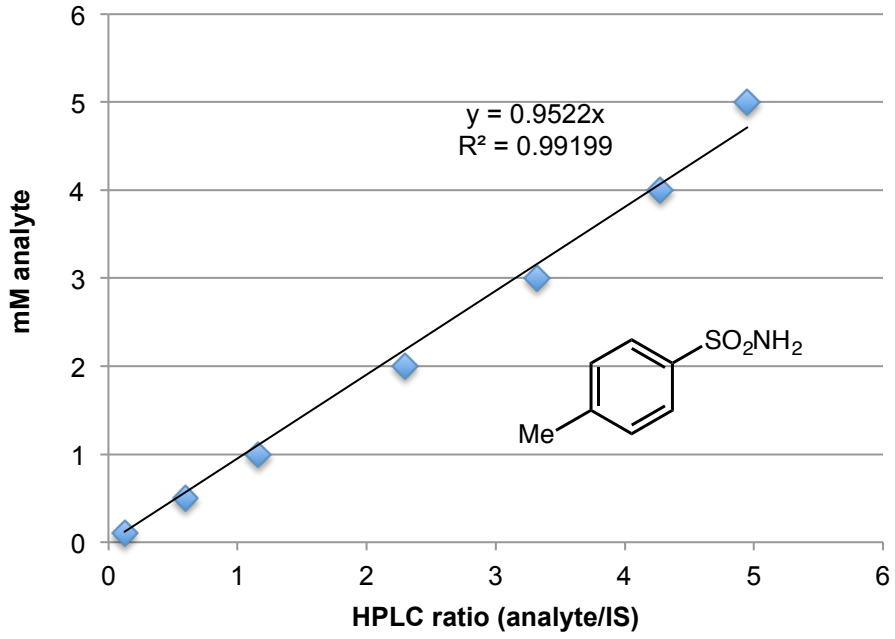

Determination of enantioselectivity.

For the determination of enantioselectivity, reaction mixtures were extracted with cyclohexane, or purified compounds were dissolved in 20% isopropanol in hexanes, and samples were analyzed by chiral SFC. Representative traces are shown below.

Assignment of absolute stereochemistry. Absolute stereochemistry was assigned by chemical synthesis of (*R*)-*N*-tosyl-1-(*p*-methoxyphenyl)ethylamine, (*S*)-*N*-tosyl-1-(*p*-tolyl)ethylamine, and (*R*)-*N*-tosyl-1-(1-naphthyl)ethylamine. Comparison to the enzymatic reactions reveals the enzymatic products to be the *R* enantiomer. Other benzylic amine products were assigned by analogy.

***N*-Tosyl-1-(*p*-methoxyphenyl)ethylamine (Table 2, entry 1).** Measured by SFC chromatography using Chiralpak AS (25% isopropanol). Racemic standard:

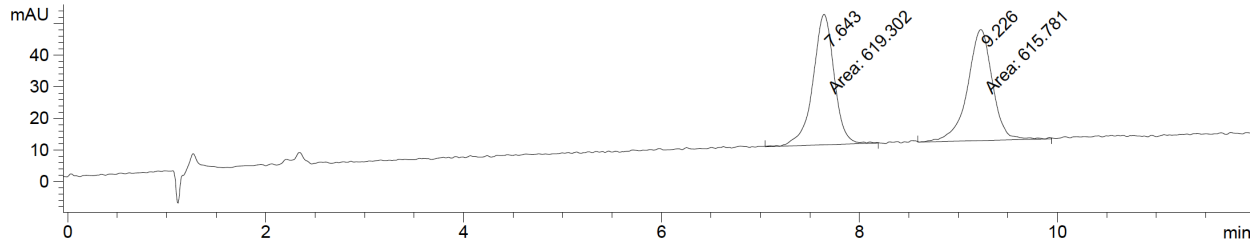

R-enantiomer, chemically prepared:

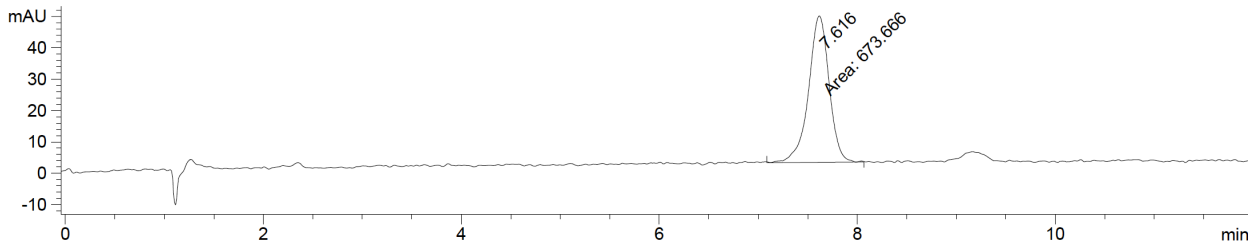

Enzymatic reaction, with $P411_{CHA}$ (>99% ee):

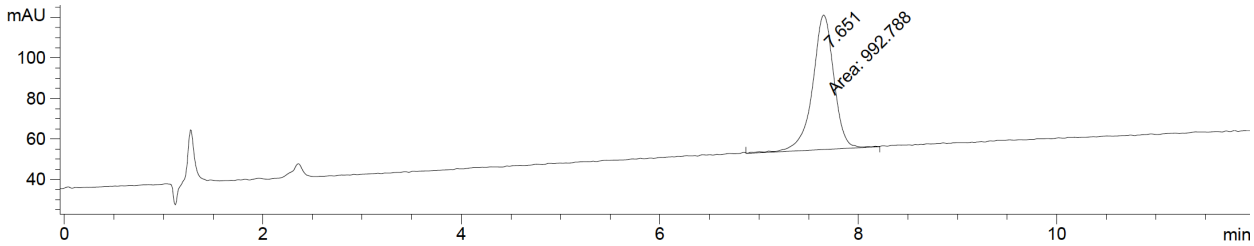

***N*-Tosyl-1-(*p*-tolyl)ethylamine (Table 2, entry 2).** Measured by SFC chromatography using Chiralpak AS (25% isopropanol). Racemic standard:

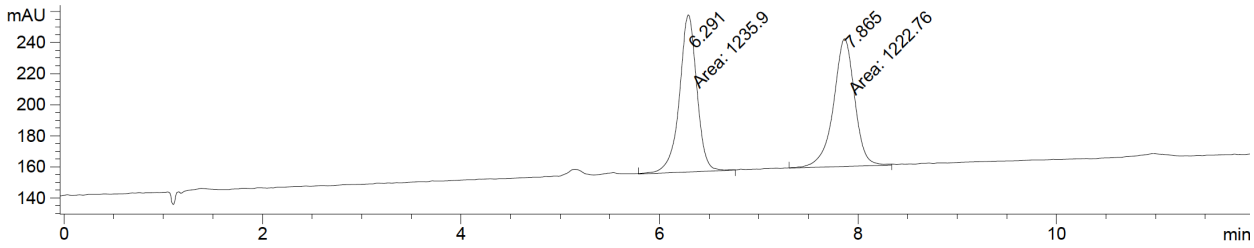

S-enantiomer, chemically prepared:

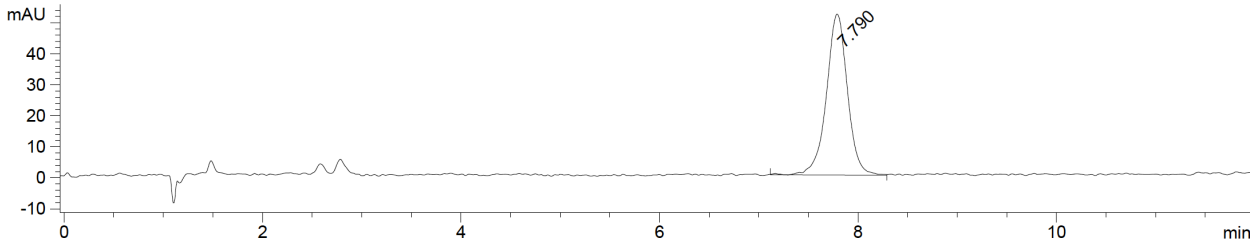

Enzymatic reaction, with P411$_{CHA}$ (>99% ee):

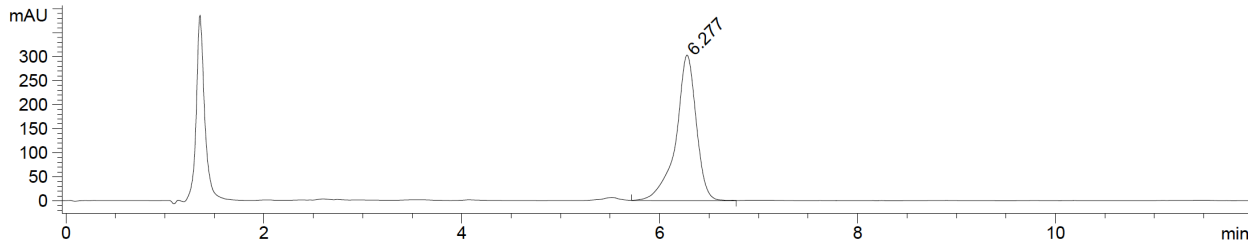

***N*-Tosyl-1-(*m*-tolyl)ethylamine (Table 2, entry 3).** Measured by SFC chromatography using Chiralpak AS (25% isopropanol). Racemic standard:

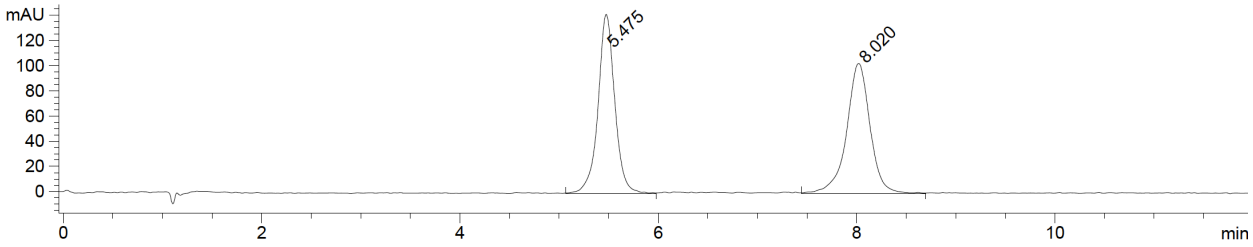

Enzymatic reaction, with $P411_{CHA}$ (>99% ee):

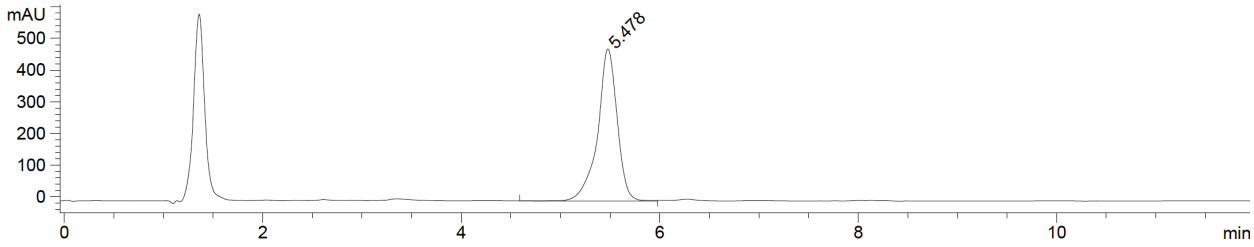

***N*-Tosyl-1-(*o*-tolyl)ethylamine (Table 2, entry 4).** Measured by SFC chromatography using Chiralpak AS (30% isopropanol). Racemic standard:

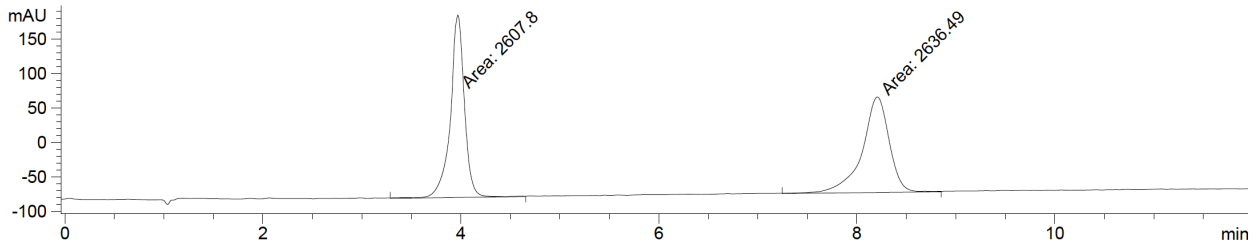

Enzymatic reaction, with $P411_{CHA}$ (87% ee):

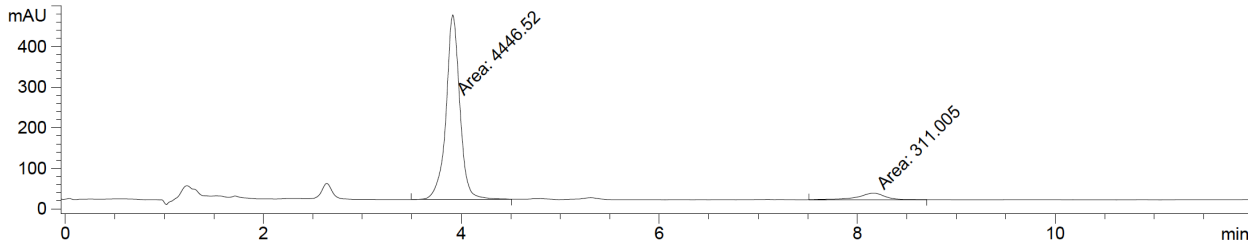

***N*-Tosyl-1-phenylethylamine (Table 2, entry 5).** Measured by SFC chromatography using Chiralpak AS (25% isopropanol). Racemic standard:

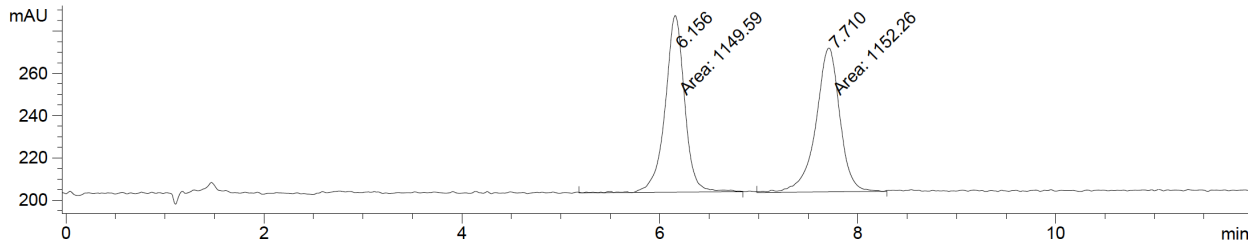

Enzymatic reaction, with $P411_{CHA}$ (>99% ee):

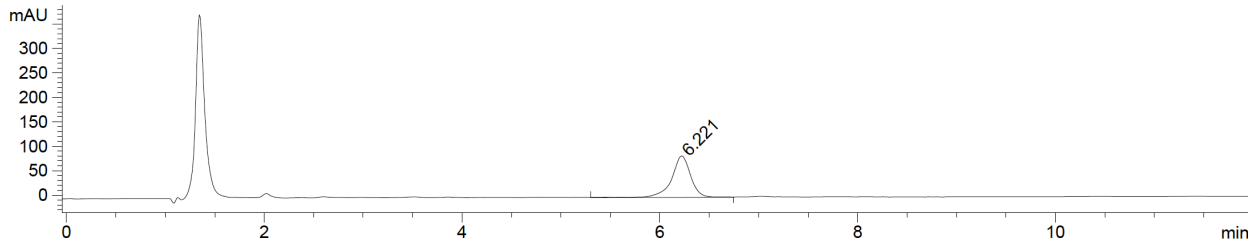

***N*-Tosyl-1-(*p*-bromophenyl)ethylamine (Table 2, entry 6).** Measured by SFC chromatography using Chiralpak AS (30% isopropanol). Racemic standard:

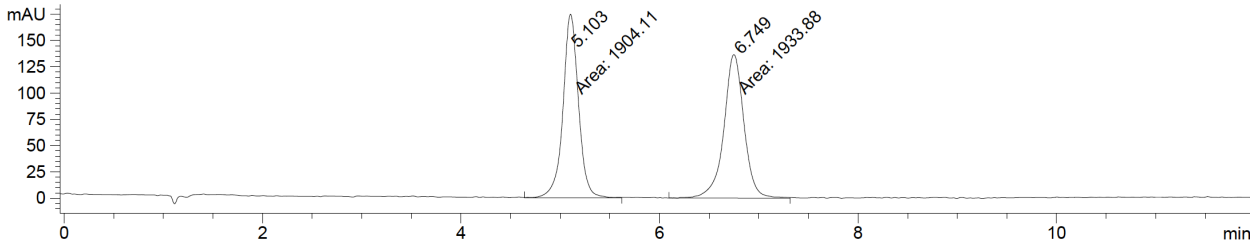

Enzymatic reaction, with $P411_{CHA}$ (>99% ee):

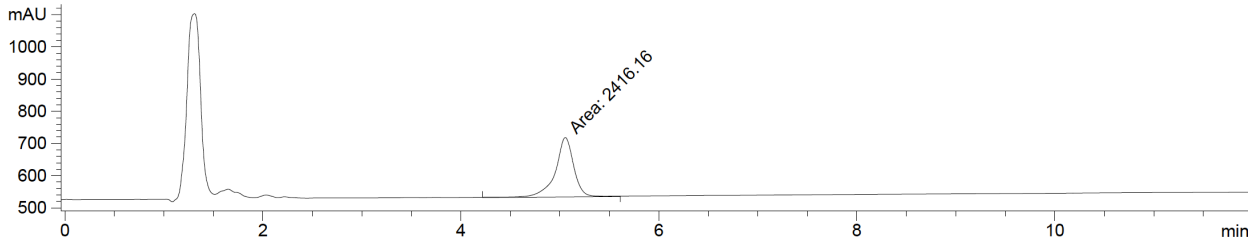

***N*-Tosyl-1-(*p*-chlorophenyl)ethylamine (Table 2, entry 7).** Measured by SFC chromatography using Chiralpak AS (25% isopropanol). Racemic standard:

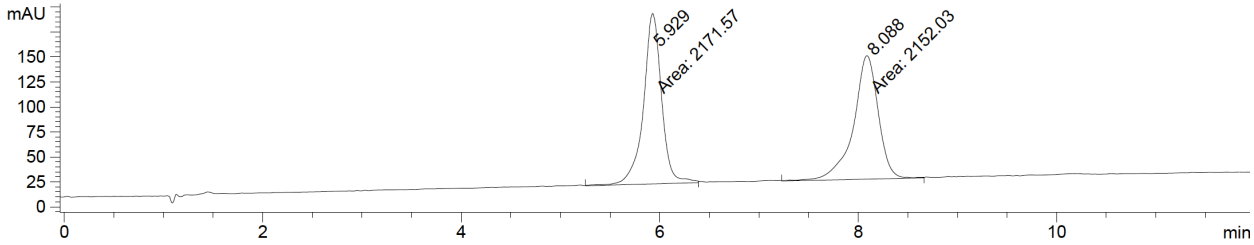

Enzymatic reaction, with $P411_{CHA}$ (>99% ee):

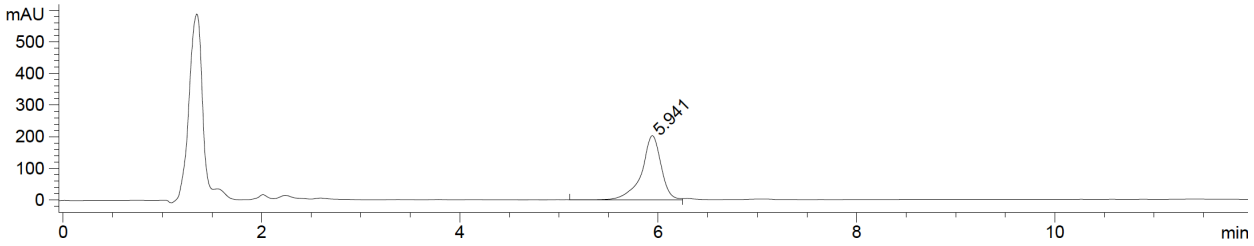

***N*-Tosyl-1-(*p*-fluorophenyl)ethylamine (Table 2, entry 8).** Measured by SFC chromatography using Chiralpak AS (25% isopropanol). Racemic standard:

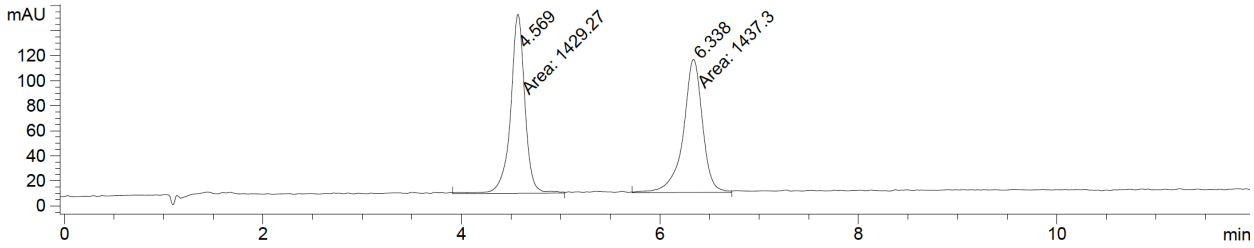

Enzymatic reaction, with $P411_{CHA}$ (>99% ee):

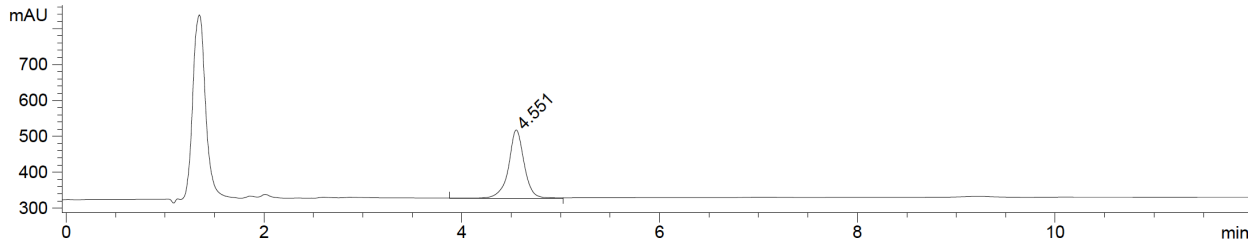

***N*-Tosyl-1-aminoindane (Table 2, entry 9).** Measured by SFC chromatography using Chiralpak AS (35% isopropanol). Racemic standard:

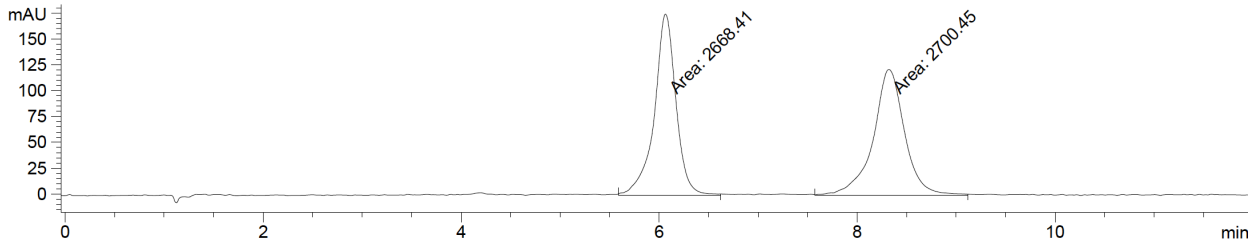

Enzymatic reaction, with $P411_{CHA}$ (96% ee):

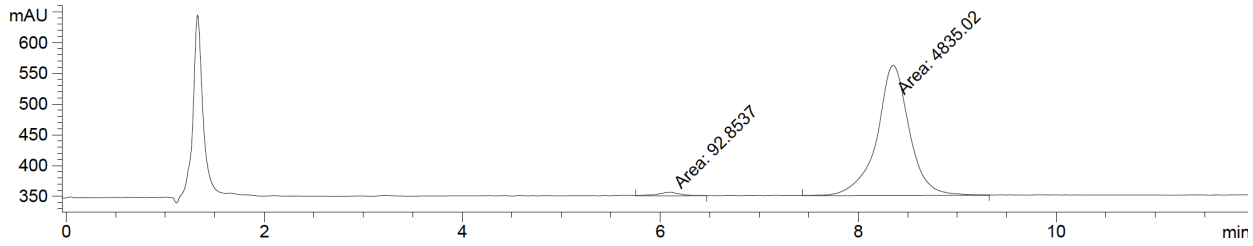

***N*-Tosyl-1-aminotetralin (Table 2, entry 10).** Measured by SFC chromatography using Chiralpak AS (40% isopropanol). Racemic standard:

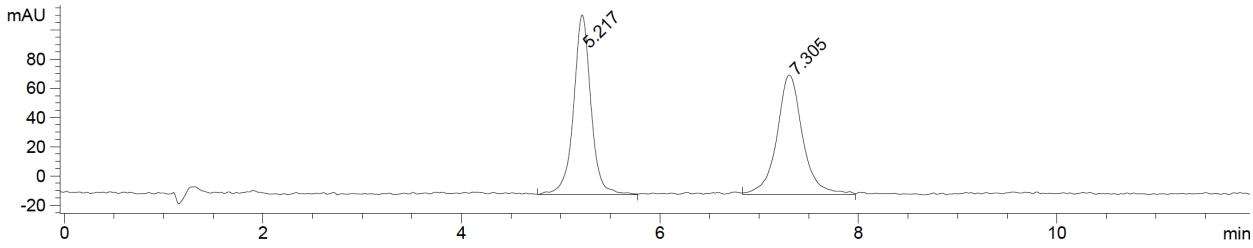

Enzymatic reaction, with $P411_{CHA}$ (95% ee):

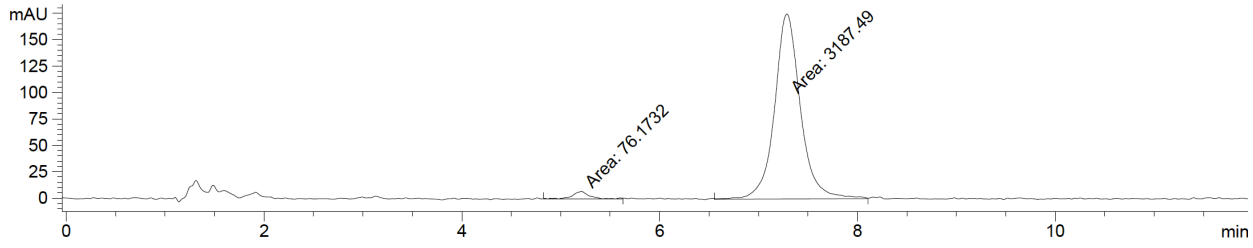

***N*-Tosyl-3-amino-2,3-dihydrobenzofuran (Table 2, entry 11).** Measured by SFC chromatography using Chiralpak AS (30% isopropanol). Racemic standard:

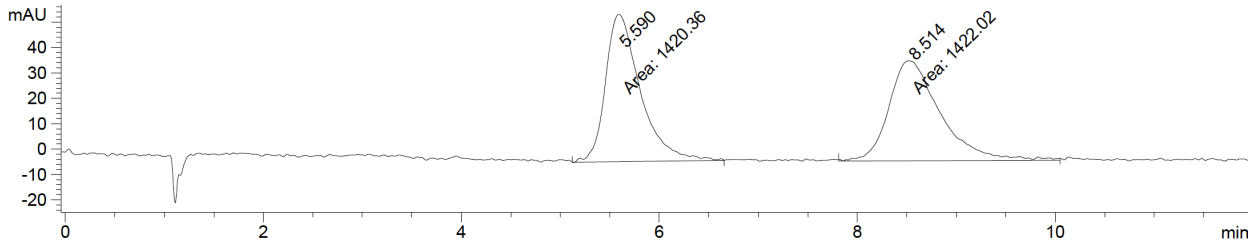

Enzymatic reaction, with $P411_{CHA}$ (92% ee):

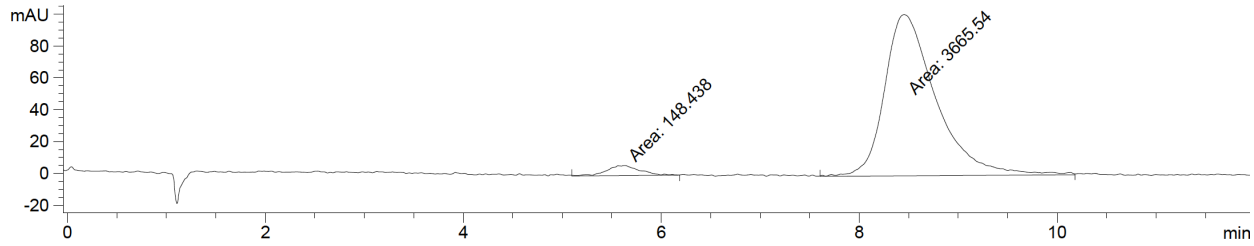

***N*-Tosyl-1-(2-naphthyl)ethylamine (Table 2, entry 12).** Measured by SFC chromatography using Chiralpak AS (40% isopropanol). Racemic standard:

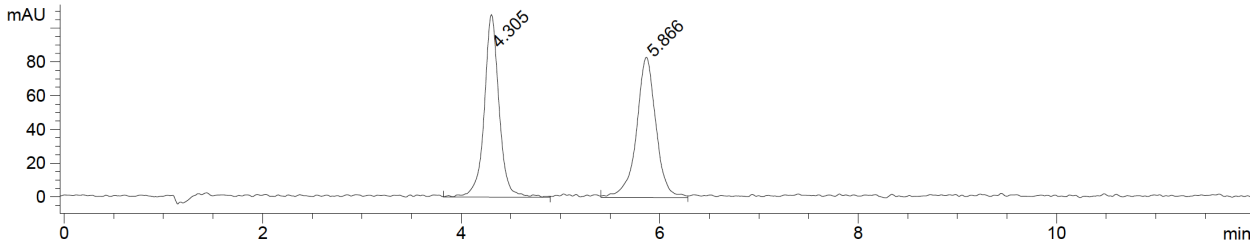

Enzymatic reaction, with $P411_{CHA}$ (>99% ee):

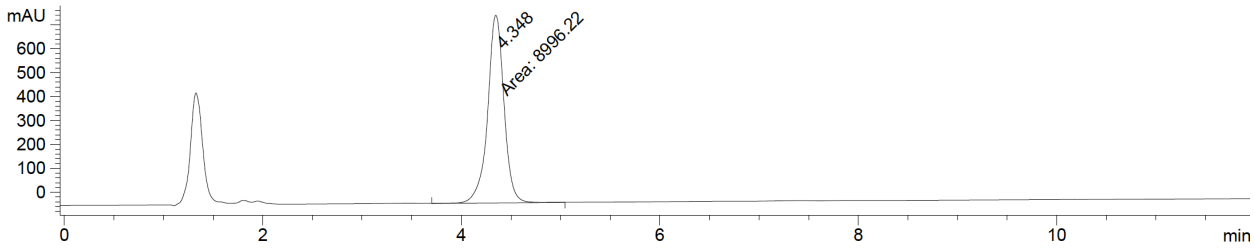

***N*-Tosyl-1-(1-naphthyl)ethylamine (Table 2, entry 13).** Measured by SFC chromatography using Chiralpak AS (40% isopropanol). Racemic standard:

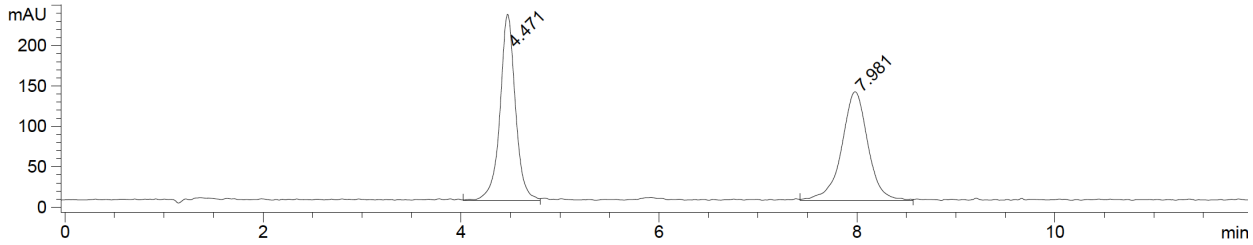

R-enantiomer, chemically prepared:

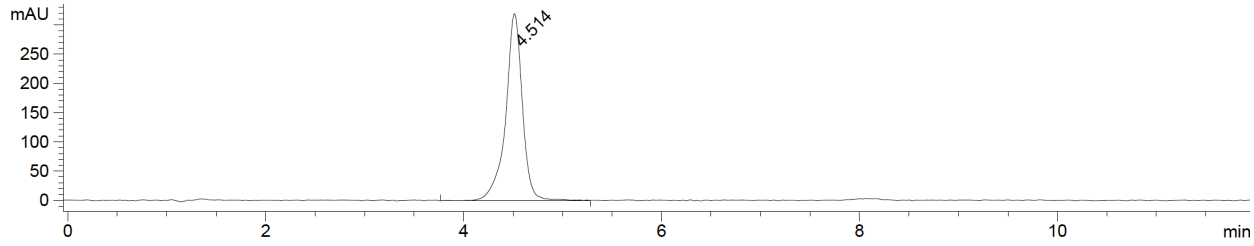

Enzymatic reaction, with $P411_{CHA}$ (>99% ee):

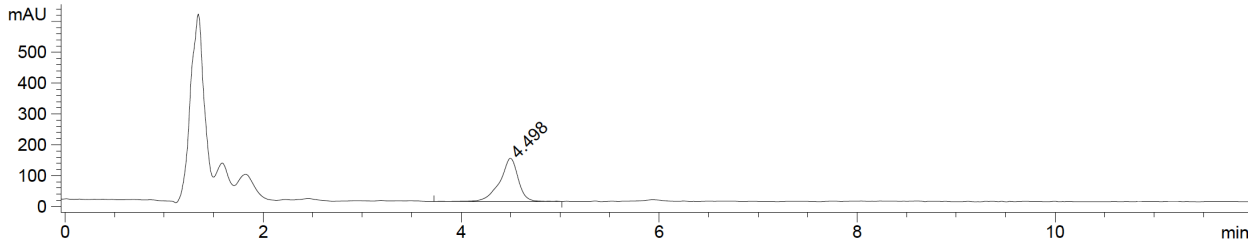

***N*-Tosyl-1-(*p*-methoxyphenyl)propylamine (Table 2, entry 14).** Measured by SFC chromatography using Chiralpak AS (25% isopropanol). Racemic standard:

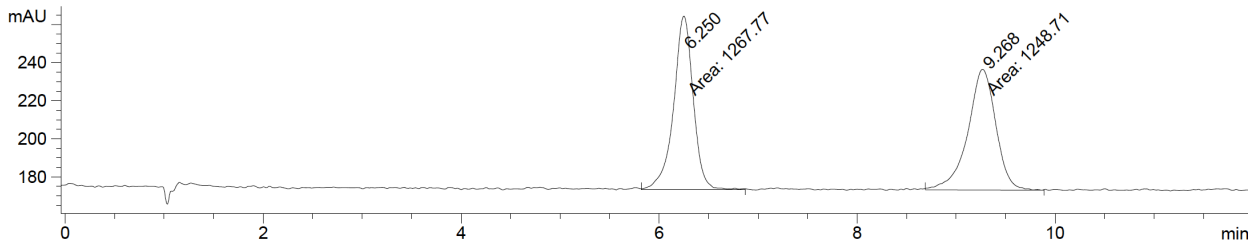

Enzymatic reaction, with P411$_{CHA}$ (>99% ee):

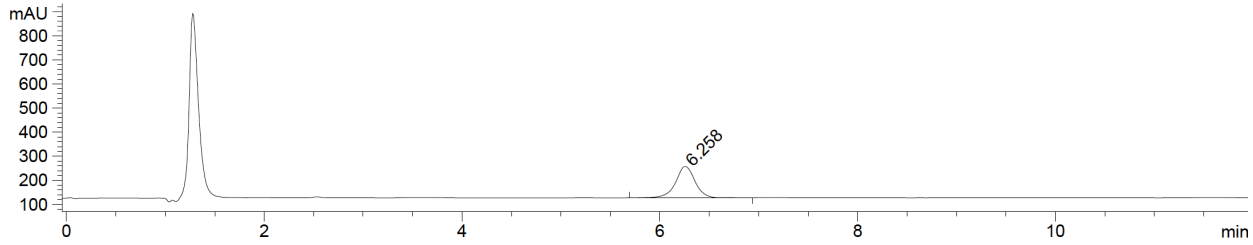

Preparative scale reactions. *E. coli* BL21 *E. cloni* cells transformed with the plasmid encoding P411$_{CHA}$ were grown overnight in 25 mL LB$_{amp}$ (37 ºC, 250 rpm). Hyperbroth medium (470 mL, 0.1 mg/mL ampicillin) in a 1-L flask was inoculated with 19 mL of the preculture and incubated at 37 ºC and 230 rpm for 2.5 h (to OD_{600} ca. 1.8). Cultures were then cooled on ice (30 min) and induced with 0.5 mM IPTG and 1.0 mM 5-aminolevulinic acid (final concentrations). Expression was conducted at room temperature (23 ºC) at 130 rpm for 16–18 h (to OD_{600} ca. 7.0). Cultures were then centrifuged (2,600 x g, 10 min, 4 ºC) and the pellets resuspended to OD_{600} = 30 in M9-N. Aliquots of the cell suspension (4 mL) were used to determine the P411 expression level after lysis by sonication. The cells (80 mL) were then combined with glucose (10 mL, 250 mM in M9-N) in a 250-mL Erlenmeyer flask and degassed by sparging with argon for at least 40 minutes. The reaction flask was then transferred into an anaerobic chamber. To the flask were added the oxygen depletion system (5 mL, 14,000 U/mL catalase and 1,000 U/mL glucose oxidase in 0.1 M KPi, pH 8.0) followed by alkane (2.5 mL, 100 mM in DMSO) and tosyl azide (2.5 mL, 200 mM in DMSO). Final concentrations were typically 2.5 mM alkane, 5.0 mM tosyl azide, and 25 mM glucose; final reaction volume was 100 mL. The flask was sealed with parafilm, removed from the anaerobic chamber, and shaken at room temperature and 130 rpm for 20 h. The reaction was quenched by adding acetonitrile (50 mL) and then centrifuged (4,000 x g, 10 min). The

supernatant was concentrated and extracted with EtOAc (3 x 25 mL). The organic layers were washed with brine (20 mL), dried over $MgSO_4$, filtered, concentrated, and purified by chromatography.

***N*-Tosyl-1-(*p*-methoxyphenyl)ethylamine.** The reaction was performed under two different conditions. To optimize yield, the reaction was performed on 0.25-mmol scale with 2.5 mM 4-ethylanisole, 5.0 mM tosyl azide, and 3.18 μM $P411_{CHA}$. The product was purified by silica gel chromatography (5 to 30% EtOAc/hexanes). Isolated 59.5 mg (78% yield, 610 TON, >99% ee). To optimize turnovers, the reaction was performed on 1.0-mmol scale with 10 mM 4-ethylanisole, 10 mM tosyl azide, and 2.80 μM $P411_{CHA}$. The product was purified by silica gel chromatography (20 to 30% EtOAc/hexanes). Isolated 103.3 mg (34% yield, 1,200 TTN, >99% ee).

***N*-Tosyl-3-amino-2,3-dihydrobenzofuran (Table 2, entry 11).** The reaction was performed on 0.25-mmol scale with 2.5 mM 2,3-dihydrobenzofuran, 5.0 mM tosyl azide, and 2.98 μM $P411_{CHA}$. The product was purified by C18 chromatography (5 to 100% MeCN/water). Isolated 15.1 mg (21% yield, 180 TON, 92% ee).

***N*-Tosyl-1,3-dihydroisobenzofuran-1-amine (Table 2, entry 16).** The reaction was performed on 0.25-mmol scale with 2.5 mM *o*-xylylene oxide, 5.0 mM tosyl azide, and 2.86 μM $P411_{CHA}$. The product was purified by preparative HPLC (50 to 100% MeCN/water). Isolated 50.7 mg (70% yield, 610 TON).

***N*-Tosyl-isochroman-1-amine (Table 2, entry 17).** The reaction was performed on 0.25-mmol scale with 2.5 mM isochroman, 5.0 mM tosyl azide, and 2.73 μM $P411_{CHA}$. The product was purified by silica gel chromatography (5 to 30% EtOAc/hexanes). Isolated 60.6 mg (80% yield, 730 TON).

Tosyl group removal. Tosyl group removal was performed by the method of Ankner and Hilmersson.[16]

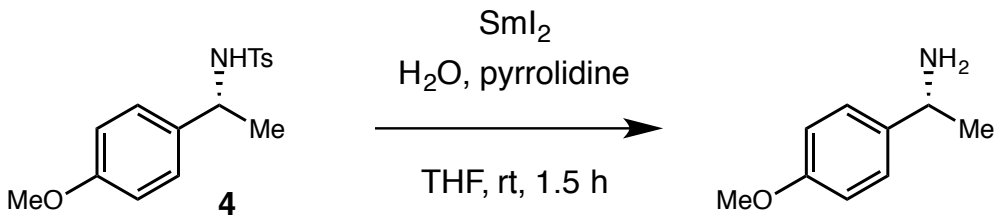

Enzymatically produced tosylamide **4** (30.5 mg, 0.1 mmol, >99% ee) in dry THF (1 mL) was added to a 0.1 M solution of SmI_2 in THF (20 mL, 2.0 mmol) at room temperature under argon. Water (108 μL, 6.0 mmol, degassed for 10 min with argon) and pyrrolidine (334 μL, 4.0 mmol, degassed for 10 min with argon) were then added. The solution was allowed to stir at room temperature under argon for 1.5 hours. The resulting reaction mixture was diluted with diethyl ether (20 mL) and quenched with a solution of potassium sodium tartrate and potassium carbonate (20 mL, 10% w/v each). The aqueous phase was extracted with three portions of diethyl ether (3 × 20 mL). The combined organics were pooled and evaporated to yield the crude amine. The crude amine was taken up in aqueous 10% HCl solution (5 mL) and washed with diethyl ether (4 × 3 mL). The aqueous layer was basified with 10% NaOH solution (5 mL) to pH 14 and extracted with dichloromethane (3 × 10 mL). The combined organic layers were dried over Na_2SO_4. Concentration gave (*R*)-1-(4-methoxyphenyl)ethanamine (9.2 mg, 61% yield) as an oil with spectral data in agreement with reported values.[17] The ee was determined to be >99% using an Agilent 7820A GC equipped with a Cyclosil-B chiral column (30 m × 0.320 mm, 0.25 μm film); method: 90–98 °C at 0.1 °C/min, 98–240 °C at 15 °C/min, 240 °C hold 5 min.

(*R*)-1-(4-methoxyphenyl)ethanamine: ^{1}H NMR (400 MHz, $CDCl_3$) δ 7.26 (d, *J* = 8.5 Hz, 2H), 6.87 (d, *J* = 8.7 Hz, 2H), 4.08 (q, *J* = 6.6 Hz, 1H), 3.80 (s, 3H), 1.59 (br s, 2H), 1.36 (d, *J* = 6.6 Hz, 3H).

Representative traces. Racemic standard, 1-(4-methoxyphenyl)ethanamine:

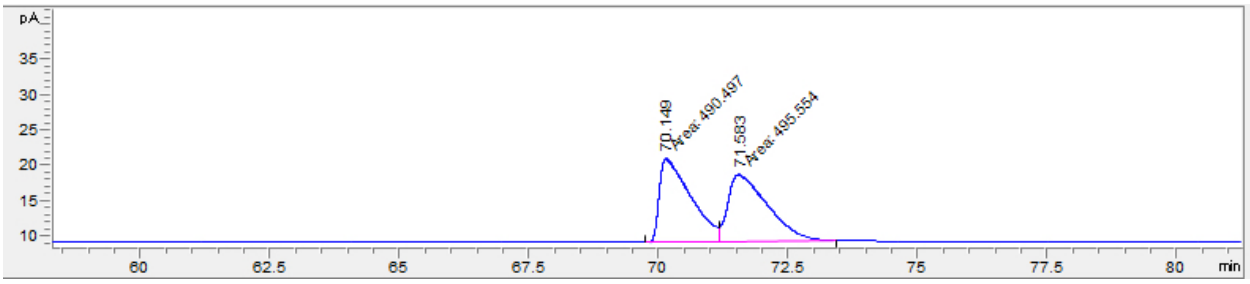

(*R*)-1-(4-methoxyphenyl)ethanamine from tosyl group removal of enzymatically produced **4**:

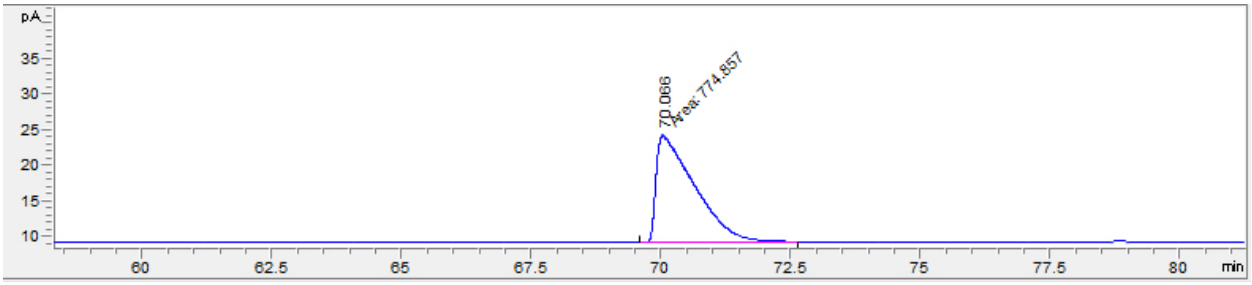

Determination of initial rates. Portions of phosphate buffer (260 μL 0.1 M KPi, pH 8.0) and NADPH (40 μL, 100 mM), or multiples thereof, were combined in a 6-mL crimp vial and degassed by sparging with argon for at least 30 minutes. Separately, glucose solution (250 mM in 0.1 M KPi, buffer pH 8.0) was also degassed in the same manner. In preparation, 2-mL crimp vials were each charged with a stir bar and the oxygen depletion system (20 μL of a stock solution containing 14,000 U/mL catalase and 1,000 U/mL glucose oxidase in 0.1 M KPi, pH 8.0). After degassing was complete, all degassed solutions, prepared 2-mL crimp vials, and purified protein (100 μM in 0.1 M KPi pH 8.0), kept on ice, were brought into the anaerobic chamber. Glucose solution (40 μL), reaction solution (300 μL), and purified protein (20 μL of 100 μM stock solution) were added to each 2-mL vial; the vials were placed on a stir plate and allowed to stir for 5 minutes. Reaction vials were then charged with alkane (10 μL, 200 mM in DMSO) and tosyl azide (10 μL, 200 mM in DMSO). Final concentrations were 5 mM alkane, 5 mM tosyl azide, 10 mM NADPH, 25 mM glucose, and 5 μM P411; final reaction volumes were 400 μL. Reactions were set up in duplicate and products quantified at 1-minute intervals by quenching with acetonitrile containing internal standard (410 μL). This mixture was then removed from the anaerobic chamber, transferred to a microcentrifuge tube, and centrifuged at 20,000 x g for 10 minutes. The supernatant was transferred to a vial and analyzed by HPLC. Rates of C–H amination and azide reduction were measured from the same reactions.

Supplementary Table 12. Initial rates of intermolecular C–H amination and azide reduction.[a]

Variant	TOF **4**	TOF $TsNH_2$ (**5**)
P-4	0.73 min^{-1}	29.1 min^{-1}
P-4 A82L	3.0 min^{-1}	13.6 min^{-1}
P-4 A82L A78V F263L	7.3 min^{-1}	12.2 min^{-1}
$P411_{CHA}$	6.4 min^{-1}	23.7 min^{-1}

[a]Variant P-4 A82L A78V F263L outperforms $P411_{CHA}$ *in vitro*, demonstrating differences in enzyme activities under whole cell versus *in vitro* conditions.

Supplementary Figure 2. Initial rates of intermolecular C–H amination of 4-ethylanisole.

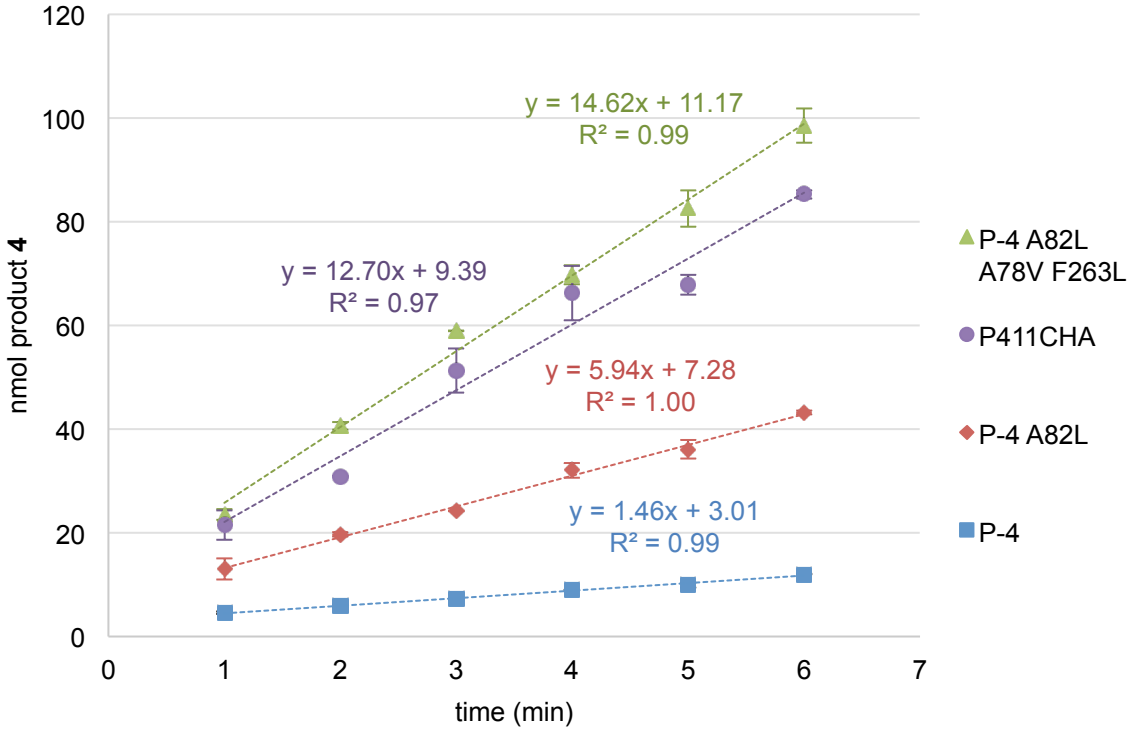

Supplementary Figure 3. Initial rates of azide reduction in the C–H amination of 4-ethylanisole.

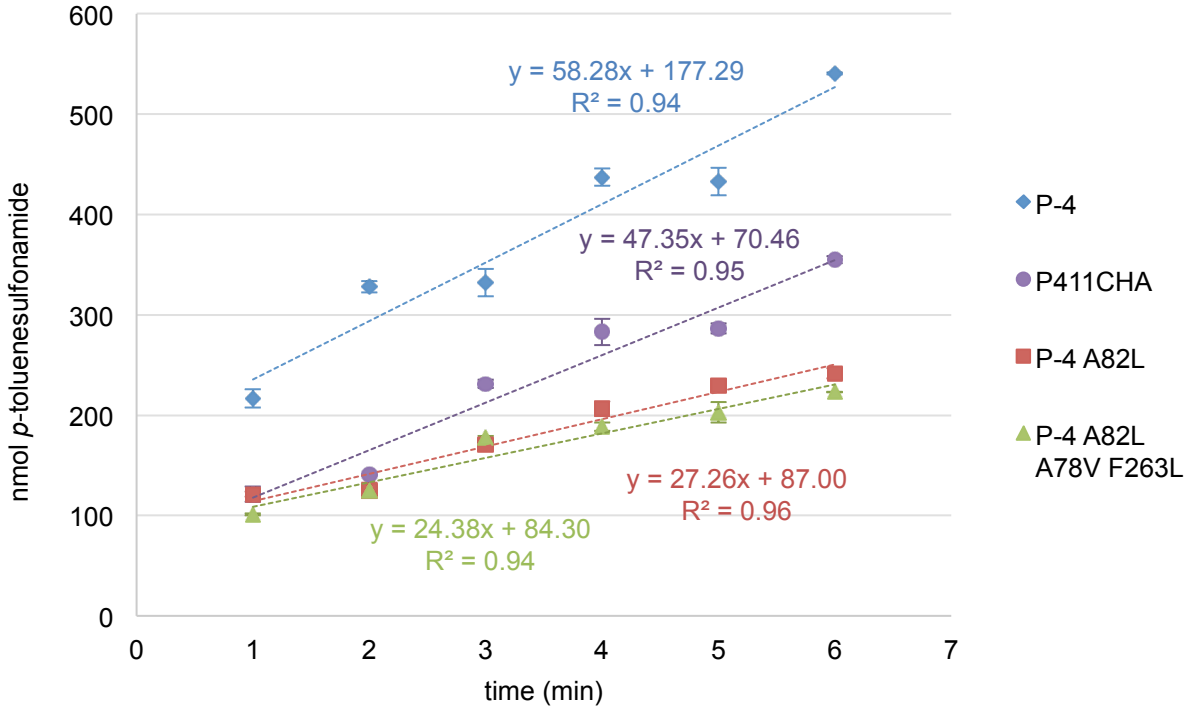

Kinetic isotope effect.

4-Ethylanisole-d_2 was prepared according the procedure of Kurita *et al.*[18] to 97% deuterium incorporation at the benzylic position. Independent rate experiments with $P411_{CHA}$ show a KIE (k_H/k_D) = 1.6; rate experiments with P-4 A82L A78V F263L show a KIE = 1.4.

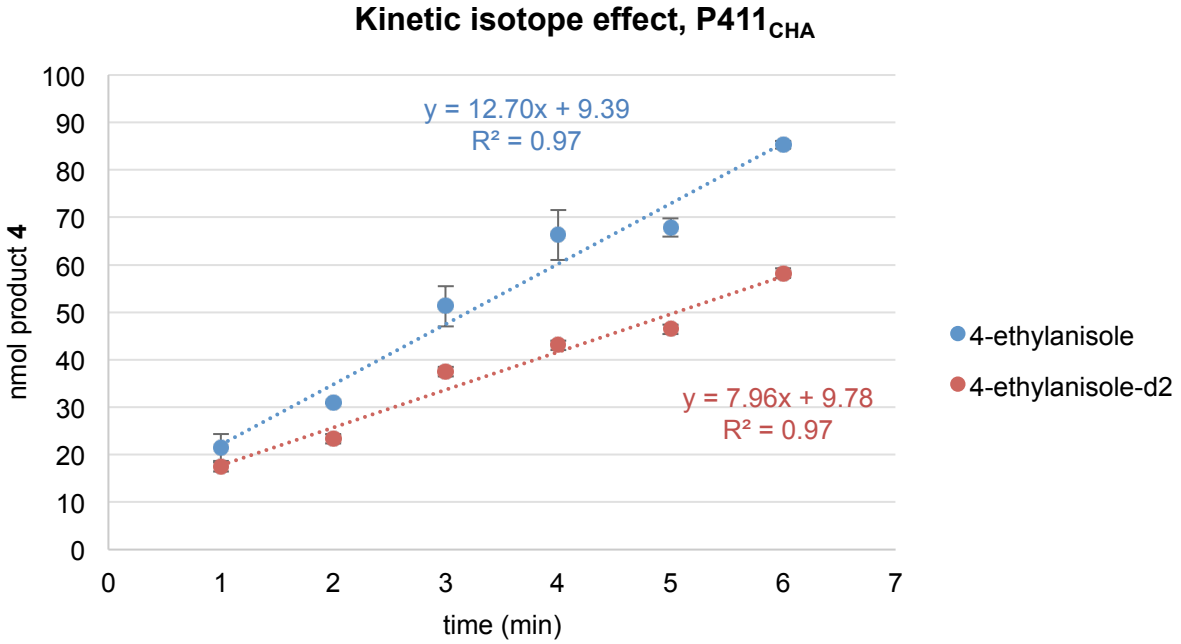

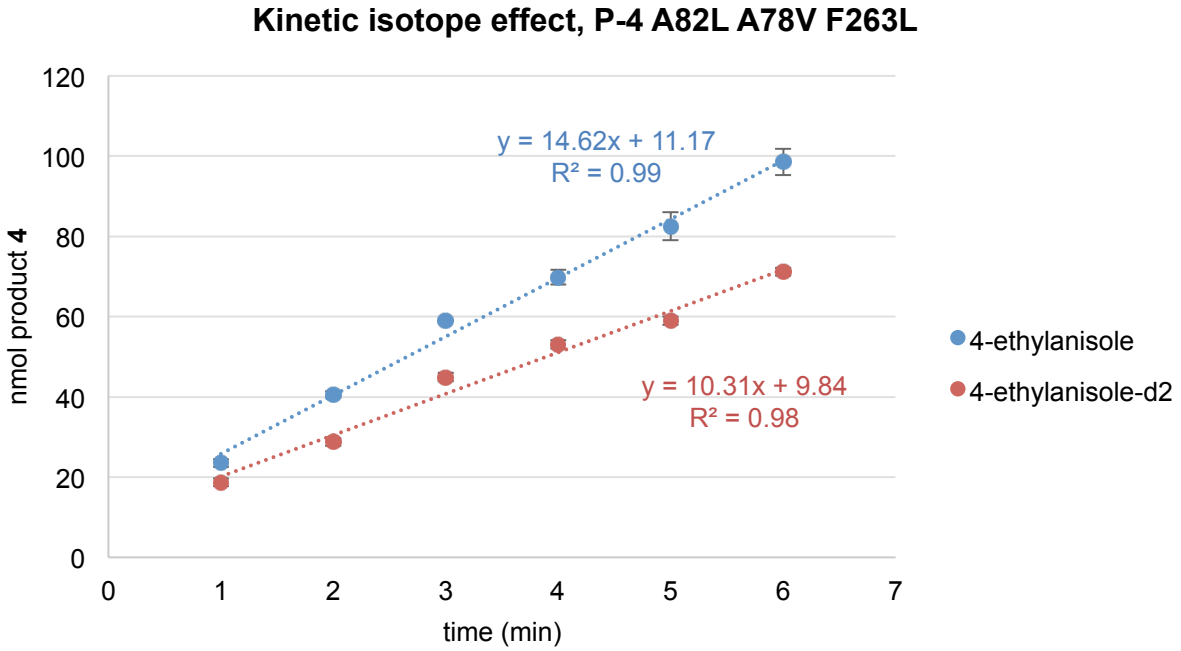

Gene sequence of cytochrome P411$_{CHA}$.

ATGACAATTAAAGAAATGCCTCAGCCAAAAACGTTTGGAGAGCTTAAAAATTTACCGTTATTAA
ACACAGATAAACCGGTTCAAGCTTTGATGAAAATTGCGGATGAATTAGGAGAAATCTTTAAATT
CGAGGCGCCTGGTCGTGTAACGCGCTACTTATCAAGTCAGCGTCTAATTAAAGAAGCATGCGAT
GAATCACGCTTTGATAAAAACTTAAGTCAAGCGCTGAAATTTGTGCGTGATTTTCTTGGAGACG
GGTTAGCCACAAGCTGGACGCATGAAAAAAATTGGAAAAAAGCGCATAATATCTTACTTCCAAG
CTTTAGTCAGCAGGCAATGAAAGGCTATCATGCGATGATGGTCGATATCGCCGTGCAGCTTGTT
CAAAAGTGGGAGCGTCTAAATGCAGATGAGCATATTGAAGTATCGGAAGACATGACACGTTTAA
CGCTTGATACAATTGGTCTTTGCGGCTTTAACTATCGCTTTAACAGCTTTTACCGAGATCAGCC
TCATCCATTTATTATAAGTATGGTCCGTGCACTGGATGAAGTAATGAACAAGCTGCAGCGAGCA
AATCCAGACGACCCAGCTTATGATGAAAACAAGCGCCAGTTTCAAGAAGATATCAAGGTGATGA
ACGACCTAGTAGATAAAATTATTGCAGATCGCAAAGCAAGGGGTGAACAAAGCGATGATTTATT
AACGCAGATGCTAAACGGAAAAGATCCAGAAACGGGTGAGCCGCTTGATGACGGGAACATTCGC
TATCAAATTATTACATTCTTACTGGCGGGACACGATGGTACAAGTGGTCTTTTATCATTTGCGC
TGTATTTCTTAGTGAAAAATCCACATGTATTACAAAAAGTAGCAGAAGAAGCAGCACGAGTTCT
AGTAGATCCTGTTCCAAGCTACAAACAAGTCAAACAGCTTAAATATGTCGGCATGGTCTTAAAC
GAAGCGCTGCGCTTATGGCCAACTGTGCCTGCGTTTTCCCTATATGCAAAAGAAGATACGGTGC
TTGGAGGAGAATATCCTTTAGAAAAAGGCGACGAAGTAATGGTTCTGATTCCTCAGCTTCACCG
TGATAAAACAGTTTGGGGAGACGATGTGGAGGAGTTCCGTCCAGAGCGTTTTGAAAATCCAAGT
GCGATTCCGCAGCATGCGTTTAAACCGTTTGGAAACGGTCAGCGTGCGTCTATCGGTCAGCAGT
TCGCTCTTCATGAAGCAACGCTGGTACTTGGTATGATGCTAAAACACTTTGACTTTGAAGATCA
TACAAACTACGAGCTCGATATTAAAGAAACTTTAAGCTTAAAACCTAAAGGCTTTGTGGTAAAA
GCAAAATCGAAAAAAATTCCGCTTGGCGGTATTCCTTCACCTAGCACTGAACAGTCTGCTAAAA
AAGTACGCAAAAAGGCAGAAAACGCTCATAATACGCCGCTGCTTGTGCTATACGGTTCAAATAT
GGGTACCGCTGAAGGAACGGCGCGTGATTTAGCAGATATTGCAATGAGCAAAGGATTTGCACCG
CAGGTCGCAACGCTTGATTCACACGCCGGAAATCTTCCGCGCGAAGGAGCTGTATTAATTGTAA
CGGCGTCTTATAACGGTCATCCGCCTGATAACGCAAAGCAATTTGTCGACTGGTTAGACCAAGC
GTCTGCTGATGAAGTAAAAGGCGTTCGCTACTCCGTATTTGGATGCGGCGATAAAAACTGGGCT
ACTACGTATCAAAAAGTGCCTGCTTTTATCGATGAAACGCTTGCCGCTAAAGGGGCAGAAAACA
TCGCTGACCGCGGTGAAGCAGATGCAAGCGACGACTTTGAAGGCACATATGAAGAATGGCGTGA
ACATATGTGGAGTGACGTAGCAGCCTACTTTAACCTCGACATTGAAAACAGTGAAGATAATAAA
TCTACTCTTTCACTTCAATTTGTCGACAGCGCCGCGGATATGCCGCTTGCGAAAATGCACGGTG
CGTTTTCAACGAACGTCGTAGCAAGCAAAGAACTTCAACAGCCAGGCAGTGCACGAAGCACGCG
ACATCTTGAAATTGAACTTCCAAAAGAAGCTTCTTATCAAGAAGGAGATCATTTAGGTGTTATT
CCTCGCAACTATGAAGGAATAGTAAACCGTGTAACAGCAAGGTTCGGCCTAGATGCATCACAGC
AAATCCGTCTGGAAGCAGAAGAAGAAAAATTAGCTCATTTGCCACTCGCTAAAACAGTATCCGT
AGAAGAGCTTCTGCAATACGTGGAGCTTCAAGATCCTGTTACGCGCACGCAGCTTCGCGCAATG
GCTGCTAAAACGGTCTGCCCGCCGCATAAAGTAGAGCTTGAAGCCTTGCTTGAAAAGCAAGCCT
ACAAAGAACAAGTGCTGGCAAAACGTTTAACAATGCTTGAACTGCTTGAAAAATACCCGGCGTG
TGAAATGAAATTCAGCGAATTTATCGCCCTTCTGCCAAGCATACGCCCGCGCTATTACTCGATT
TCTTCATCACCTCGTGTCGATGAAAAACAAGCAAGCATCACGGTCAGCGTTGTCTCAGGAGAAG
CGTGGAGCGGATATGGAGAATATAAAGGAATTGCGTCGAACTATCTTGCCGAGCTGCAAGAAGG
AGATACGATTACGTGCTTTATTTCCACACCGCAGTCAGAATTTACGCTGCCAAAAGACCCTGAA
ACGCCGCTTATCATGGTCGGACCGGGAACAGGCGTCGCGCCGTTTAGAGGCTTTGTGCAGGCGC
GCAAACAGCTAAAAGAACAAGGACAGTCACTTGGAGAAGCACATTTATACTTCGGCTGCCGTTC
ACCTCATGAAGACTATCTGTATCAAGAAGAGCTTGAAAACGCCCAAAGCGAAGGCATCATTACG
CTTCATACCGCTTTTTCTCGCATGCCAAATCAGCCGAAAACATACGTTCAGCACGTAATGGAAC

AAGACGGCAAGAAATTGATTGAACTTCTTGATCAAGGAGCGCACTTCTATATTTGCGGAGACGG
AAGCCAAATGGCACCTGCCGTTGAAGCAACGCTTATGAAAAGCTATGCTGACGTTCACCAAGTG
AGTGAAGCAGACGCTCGCTTATGGCTGCAGCAGCTAGAAGAAAAAGGCCGATACGCAAAAGACG
TGTGGGCTGGG

Amino acid sequence of cytochrome P411$_{CHA}$.

MTIKEMPQPKTFGELKNLPLLNTDKPVQALMKIADELGEIFKFEAPGRVTRYLSSQRLIKEACD
ESRFDKNLSQALKFVRDFLGDGLATSWTHEKNWKKAHNILLPSFSQQAMKGYHAMMVDIAVQLV
QKWERLNADEHIEVSEDMTRLTLDTIGLCGFNYRFNSFYRDQPHPFIISMVRALDEVMNKLQRA
NPDDPAYDENKRQFQEDIKVMNDLVDKIIADRKARGEQSDDLLTQMLNGKDPETGEPLDDGNIR
YQIITFLLAGHDGTSGLLSFALYFLVKNPHVLQKVAEEAARVLVDPVPSYKQVKQLKYVGMVLN
EALRLWPTVPAFSLYAKEDTVLGGEYPLEKGDEVMVLIPQLHRDKTVWGDDVEEFRPERFENPS
AIPQHAFKPFGNGQRASIGQQFALHEATLVLGMMLKHFDFEDHTNYELDIKETLSLKPKGFVVK
AKSKKIPLGGIPSPSTEQSAKKVRKKAENAHNTPLLVLYGSNMGTAEGTARDLADIAMSKGFAP
QVATLDSHAGNLPREGAVLIVTASYNGHPPDNAKQFVDWLDQASADEVKGVRYSVFGCGDKNWA
TTYQKVPAFIDETLAAKGAENIADRGEADASDDFEGTYEEWREHMWSDVAAYFNLDIENSEDNK
STLSLQFVDSAADMPLAKMHGAFSTNVVASKELQQPGSARSTRHLEIELPKEASYQEGDHLGVI
PRNYEGIVNRVTARFGLDASQQIRLEAEEEKLAHLPLAKTVSVEELLQYVELQDPVTRTQLRAM
AAKTVCPPHKVELEALLEKQAYKEQVLAKRLTMLELLEKYPACEMKFSEFIALLPSIRPRYYSI
SSSPRVDEKQASITVSVVSGEAWSGYGEYKGIASNYLAELQEGDTITCFISTPQSEFTLPKDPE
TPLIMVGPGTGVAPFRGFVQARKQLKEQGQSLGEAHLYFGCRSPHEDYLYQEELENAQSEGIIT
LHTAFSRMPNQPKTYVQHVMEQDGKKLIELLDQGAHFYICGDGSQMAPAVEATLMKSYADVHQV
SEADARLWLQQLEEKGRYAKDVWAG

Crystallization, X-ray data collection, and protein structure determination of P-4 A82L A78V F263L heme domain. The construct employed for crystallization is the heme domain of variant P-4 A82L A78V F263L (residues 1 to 463 of the holoprotein, followed by an *Xho*I site and a C-terminal His-tag). The amino acid sequence is:

```
MTIKEMPQPKTFGELKNLPLLNTDKPVQALMKIADELGEIFKFEAPGRVTRYLSSQRLIKEACD
ESRFDKNLSQALKFVRDFLGDGLATSWTHEKNWKKAHNILLPSFSQQAMKGYHAMMVDIAVQLV
QKWERLNADEHIEVSEDMTRLTLDTIGLCGFNYRFNSFYRDQPHPFIISMVRALDEVMNKLQRA
NPDDPAYDENKRQFQEDIKVMNDLVDKIIADRKARGEQSDDLLTQMLNGKDPETGEPLDDGNIR
YQIITFLLAGHEGTSGLLSFALYFLVKNPHVLQKVAEEAARVLVDPVPSYKQVKQLKYVGMVLN
EALRLWPTVPAFSLYAKEDTVLGGEYPLEKGDEVMVLIPQLHRDKTVWGDDVEEFRPERFENPS
AIPQHAFKPFGNGQRASIGQQFALHEATLVLGMMLKHFDFEDHTNYELDIKETLSLKPKGFVVK
AKSKKIPLGGIPSPSTLEHHHHHH
```

The heme domain of variant P-4 A82L A78V F263L was crystalized by vapor diffusion. A 1:1 mixture of protein stock (22 mg/mL protein in 25 mM tris-HCl, 25 mM NaCl, pH 7.5 buffer) and mother liquor were combined in 24-well sitting drop plates (Hampton Research). The crystals were grown at room temperature over a span of 4–10 days. Crystals formed in 0.1 M bis-tris pH 4.0–5.0, 13% PEG 3350, 0.2 M NaHCOO. Data was collected on a crystal that formed under the following conditions: 0.1 M Bis-tris pH 5.0, 13% PEG 3350, 0.2 M NaHCOO. Crystals were cryo-protected by immersion into well solution with 25% glycerol before being flash-frozen in liquid N_2. Diffraction data were collected on the Stanford Synchrotron Radiation Laboratory Beamline 12-2. Data was processed using XDS[19] in the space group $P2_12_12$ and scaled using AIMLESS[20] to 1.70-Å resolution.

The structure of P-4 A82L A78V F263L was solved by molecular replacement using PHASER, as implemented in CCP4, using the $P411_{BM3}$-CIS T438S I263F structure (PDB ID: 4WG2) as the search model. Model building was performed in Coot and restrained refinement performed using Refmac5.[21,22] TLS operators were included in the last round of refinement.[23] Model quality was assessed with the MolProbity online server.[24] Crystallographic and model statistics are described in Supplementay Table 13.

Supplementary Table 13. X-ray crystallography analysis of cytochrome $P411_{BM3}$ P-4 A82L A78V F263L.

Data collection	
Protein	Cytochrome $P411_{BM3}$ P-4 A82L A78V F263L
PDB ID	5UCW
Beamline	SSRL 12.2[a]
Space group	$P2_12_12$
Cell dimensions	
a, *b*, *c* (Å)	123.9, 127.0, 62.6
α, β, γ (°)	90.0, 90.0, 90.0
Wavelength	0.9795
Resolution (Å) (last bin A)	40.0 – 1.70
Last bin (Å)	1.73 – 1.70
R_{meas} (%)[b]	5.5 (262.2)
R_{pim} (%)[b]	1.5 (69.8)
$CC_{1/2}$[b]	1.00 (0.593)
$< I / \sigma I >$[b]	23.9 (1.3)
Completeness (%)[b]	99.8 (100.0)
No. of observations	1,462,616
No. of unique reflections[b]	108,841 (5,345)
Redundancy[b]	13.4 (13.8)
Refinement	
Resolution (Å)	40.0 – 1.70
Final bin (Å)	1.744 – 1.700
No. of reflections	103,324
No. of reflections test set	5,400 (5.0%)
R_{work} / R_{free}[b]	18.9 / 22.3 (34.4 / 33.1)
Total no. atoms (non-hydrogen)	7,709
Average *B*-factor (Å^2)	42.2
RMSD	
Bond lengths (Å)	0.012
Bond angles (°)	1.44
Ramachandran plot[c]	
Favored (%)	97.3
Additionally allowed (%)	2.7
Outliers (%)	0.0
MolProbity	
Clashscore[c]	2.76 (99th percentile)
Molprobity score[c]	1.29 (97th percentile)

[a]SSRL, Stanford Synchotron Radiation Lightsource. [b]Highest-resolution shell is shown in parentheses. [c]As determined by MolProbity.

R_{work} is ||Fo – Fc|| / Fo, where Fo is an observed amplitude and Fc a calculated amplitude; R_{free} is the same statistic calculated over a 5.0% subset of the data that has not been included during refinement.

Structure of P-4 A82L A78V F263L.

The structure of P-4 A82L A78V F263L adopts the P450 closed conformation, aligning well with the two previously obtained cytochrome P411 structures (PDB IDs 4WG2 and 4H23) as well as with $P450_{BM3}$ wild type in complex with *N*-palmitoylglycine (1JPZ).[25]

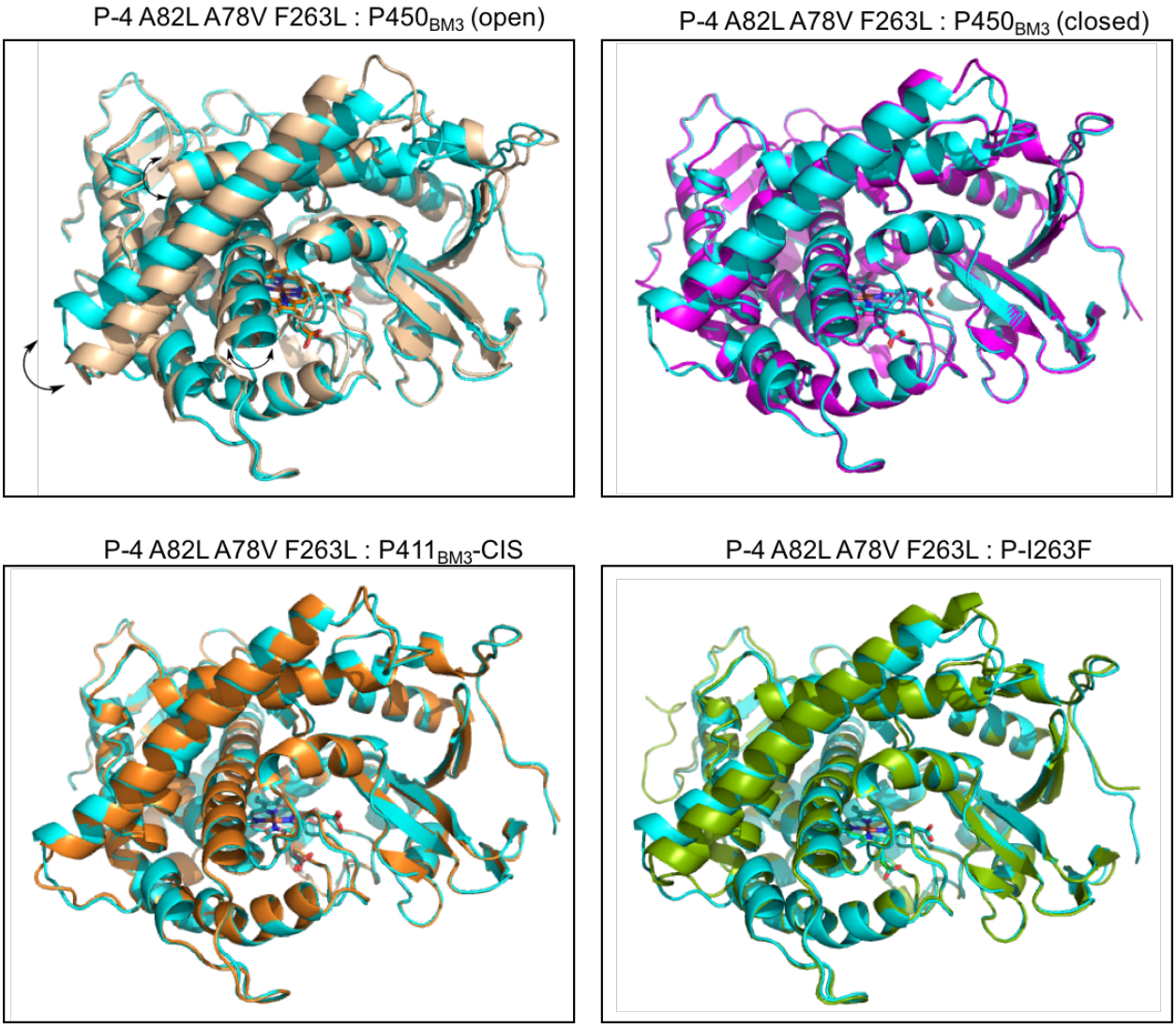

Supplementary Figure 4. Heme domain protein alignments of cytochrome $P411_{BM3}$ P-4 A82L A78V F263L with wild type $P450_{BM3}$ and other $P411_{BM3}$ structures. Top panels show alignments of $P411_{BM3}$ P-4 A82L A78V F263L (cyan) with open (substrate free) form of wild type $P450_{BM3}$ (tan, PDB 2IJ2) and closed (substrate bound) form of wild-type $P450_{BM3}$ (magenta, PDB 1JPZ). Large movements of the I, F, and G helices are observed when comparing P-4 A82L A78V

F263L with the open form of wild-type $P450_{BM3}$ (arrows); the position of these helices align more closely with the closed form of wild type $P450_{BM3}$. Bottom panels show alignments of $P411_{BM3}$ P-4 A82L A78V F263L (cyan) with previously obtained $P411_{BM3}$ structures, $P411_{BM3}$-CIS (orange, PDB 4H23) and P-I263F (green, PDB 4WG2). No significant structural changes are observed. Protein alignments were carried about using the align tool of PyMOL (PyMOL Molecular Graphics System, Version 1.3, Schrodinger LLC).

The structure of P-4 A82L A78V F263L was compared closely to that of P-I263F (4WG2), as differences between these structures may reflect features that account for the emergence of intermolecular C–H amination activity: these two variants differ by only six mutations, yet P-4 A82L A78V F263L is a competent intermolecular amination catalyst while P-I263F gives only trace product. Comparisons between structures were made by performing pairwise alignments using secondary structure matching (SSM) in Coot or aligning backbone atoms in PyMOL (zero cycles). Globally, the largest differences in the position of protein backbone atoms are observed between the F and G helices and the F/G and G/H loops, which are known to be the most variable regions of P450s (Supplementary Fig. 5).[26] Volumes of the heme distal pocket were estimated by the CASTp server using a 1.4-Å probe.[27] Estimated volumes for P-4 A82L A78V F263L were 1489 and 1411 $Å^3$ for the two chains; estimated volumes for P-I263F (4WG2) were 1422, 1655, and 1737 $Å^3$ for the three chains.

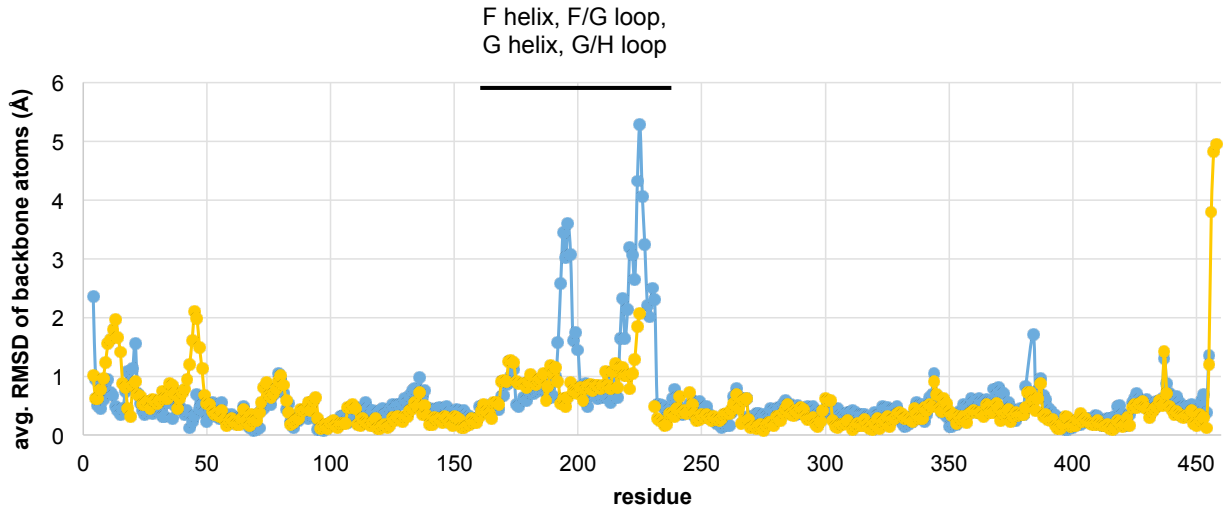

Supplementary Figure 5. Representative plots of r.m.s. difference between the backbone atoms of P-4 A82L A78V F263L and P-I263F (PDB 4WG2). Blue: comparison of molecule A in P-4 A82L A78V F263L and molecule A in P-I263F. Yellow: comparison of molecule B of P-4 A82L A78V F263L and molecule C of P-I263F.

Local differences within the distal heme pocket were also observed between P-4 A82L A78V F263L and P-I263F. Notably, the mutation A268G of P-4 A82L A78V F263L displays a ~0.8-Å movement of C(α) closer to C2 of the heme cofactor; simple mutation of G268 back to alanine in P-4 A82L A78V F263L, using Coot, shows steric clash of the methyl side chain with the heme, suggesting the protein would not be able to adopt this conformation with alanine at this position. The backbone of the B' helix (site of the mutations A82L and A78V) shifts by 0.6 to 0.9 Å toward the distal heme face. In general, the backbones of the I-helices between the two structures align well, with the exception of the backbone nitrogen of A264, which shifts by 0.7 Å from its position in P-I263F to accommodate the F263L mutation in P-4 A82L A78V F263L. Other notable residues in the P-4 A82L A78V F263L structure include P329, which has changed to endo conformation from exo in P-I263F, and L437, which has significantly changed torsion angles.

Docking simulations.

Docking simulations were performed using Autodock Vina and the crystal structure of P-4 A82L A78V F263L.[28] BioLuminate (Schrödinger) was used to draw ligands, and AutoDockTools was used to generate PDBQT files. To simulate the orientation of the nitrenoid intermediate, a ligand was created having the nitrogen atom linked to the iron of the heme cofactor; the Fe–N distance was set to 1.8 Å.[29] Docking this ligand into the cofactor-free structure gave an output having the heme approximately in the same orientation as that observed in the crystal structure (Supplementary Fig. 6). The arene and *p*-methyl group of the reagent pack against the I helix, making interactions with F263 (3.7 Å), A264 (3.9 Å), and E267 (3.5 Å). Other residues at close distances to the ligand are L181 on the F helix, and A87, V328, and S438 on active-site loops.

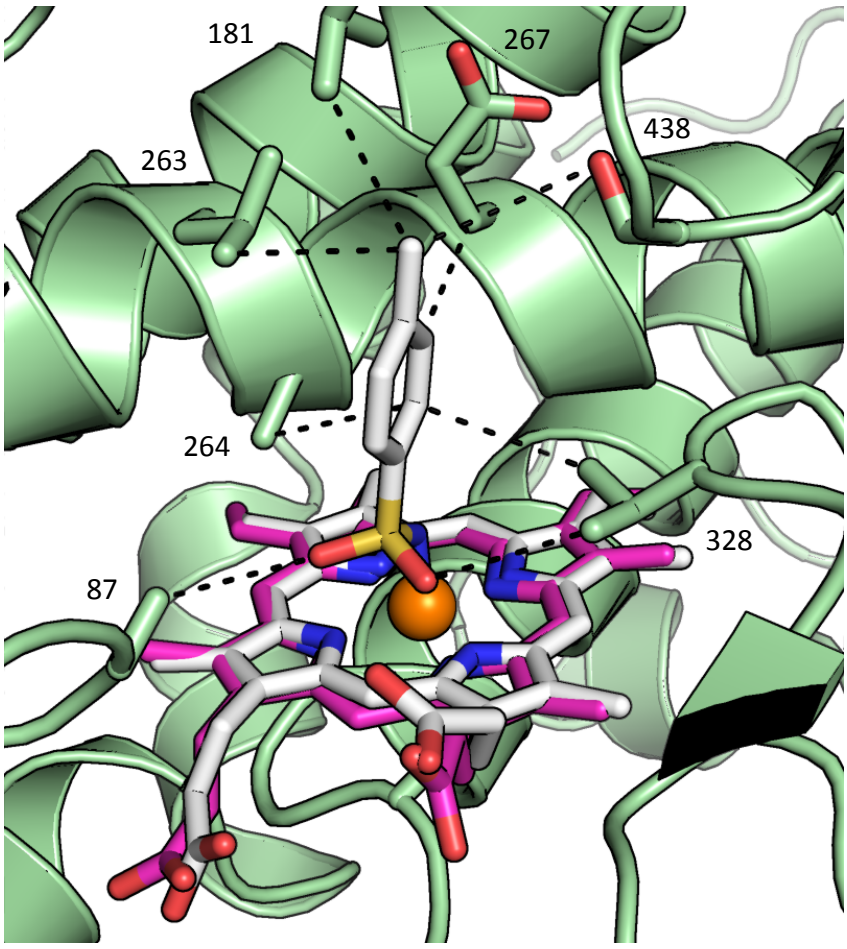

Supplementary Figure 6. Docking of the metal nitrenoid/heme complex into the active site of P411 variant P-4 A82L A78V F263L. The docked ligand is shown in white; the orientation of the heme in the crystal structure is shown in magenta. Distances of closest contact between the ligand and active site residues are shown as black dashes.

To simulate the conformation of the nitrenoid and alkane reagents during the C–H amination event, we attempted to dock the product of amination. Docking of the product (*R*)-**4** into the structure of the cofactor-bound enzyme, however, did not reveal binding modes relevant to the bond-forming step (i.e., Fe–N distances of all outputs were >6.5 Å). Therefore, the product (*R*)-**4** was linked to the heme via nitrogen and this ligand docked into the cofactor-free structure (as described above for the nitrenoid model). The Fe–N distance was set to 2.1 Å, as observed in imidazole-bound P450 structures.[30] Only outputs showing the correct orientation of the heme were considered. Various simulations, with the ligand docked into either chain of the protein, with different configurations at nitrogen, or with alternative substrates, repeatedly identified two general binding modes for the product. In one mode, the sulfonamide occupies the site near the I helix observed in the nitrenoid model (above), while the anisole ring is oriented toward the B' helix, specifically residue L75 (Supplementary Fig. 7).

In the other binding mode, the positions of the two arenes are roughly swapped: the anisole is oriented against the I helix, and the sulfonamide arene is positioned close to the B' helix (Supplementary Figure 8). Residues that make contact with the ligand in both orientations include L75, A87, L181, L263, A264, E267, V328, and S438. Several of these residues were mutated in the evolutionary lineage from P-I263F to $P411_{CHA}$ (residues 87, 263, 267, 328). In both orientations, the ligand is contacted on all sides by protein side chains, showing how the enzyme may potentially enforce productive binding modes for catalysis. Docking simulations performed with varying Fe–N bond lengths (1.8 Å to 2.4 Å) also produced similar orientations of the ligand.

The docking simulations with the heme/*R*-(**4**) ligand also show a shift of the heme away from the I helix (by up to ~1.5 Å), presumably to minimize clashes between the ligand and helix residues. However, substrate binding to P450s is known to induce a movement of the I helix away from the heme;[25,31] such movement of the protein backbone may be required in these P411 variants during catalysis. A better understanding of substrate binding modes will require further computational or co-crystallization studies.

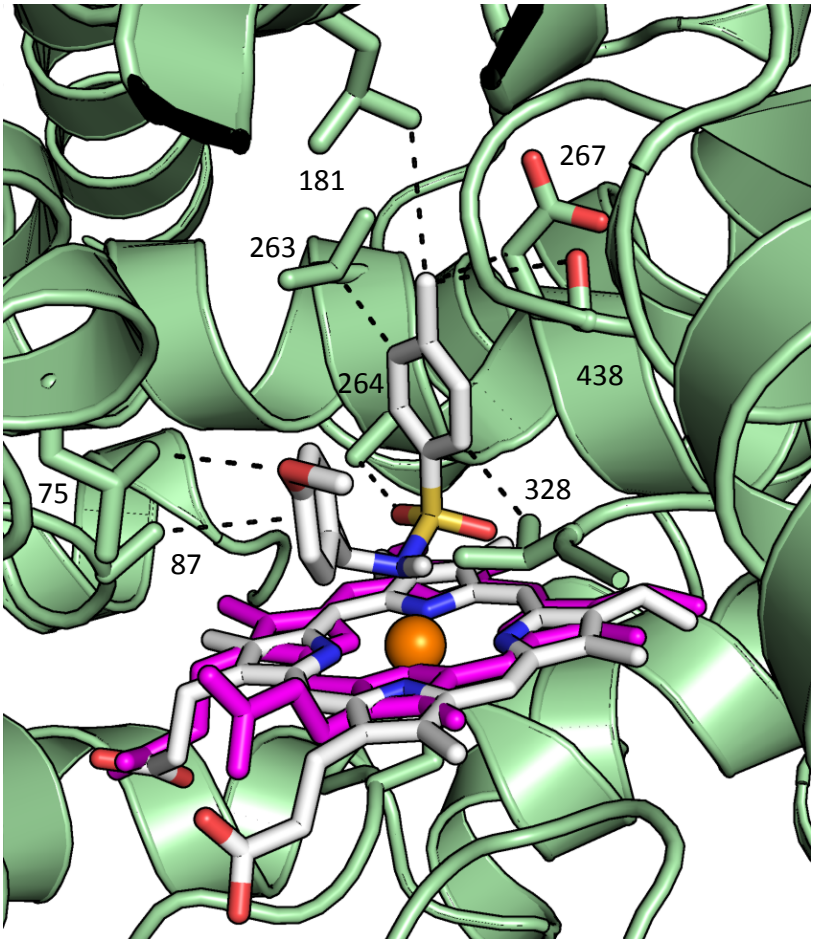

Supplementary Figure 7. Docking of the (*R*)-**4**/heme complex into the active site of P411 variant P-4 A82L A78V F263L, first binding mode. The docked ligand is shown in white; the orientation of the heme in the crystal structure is shown in magenta. Distances of closest contact between the ligand and active site residues are shown as black dashes.

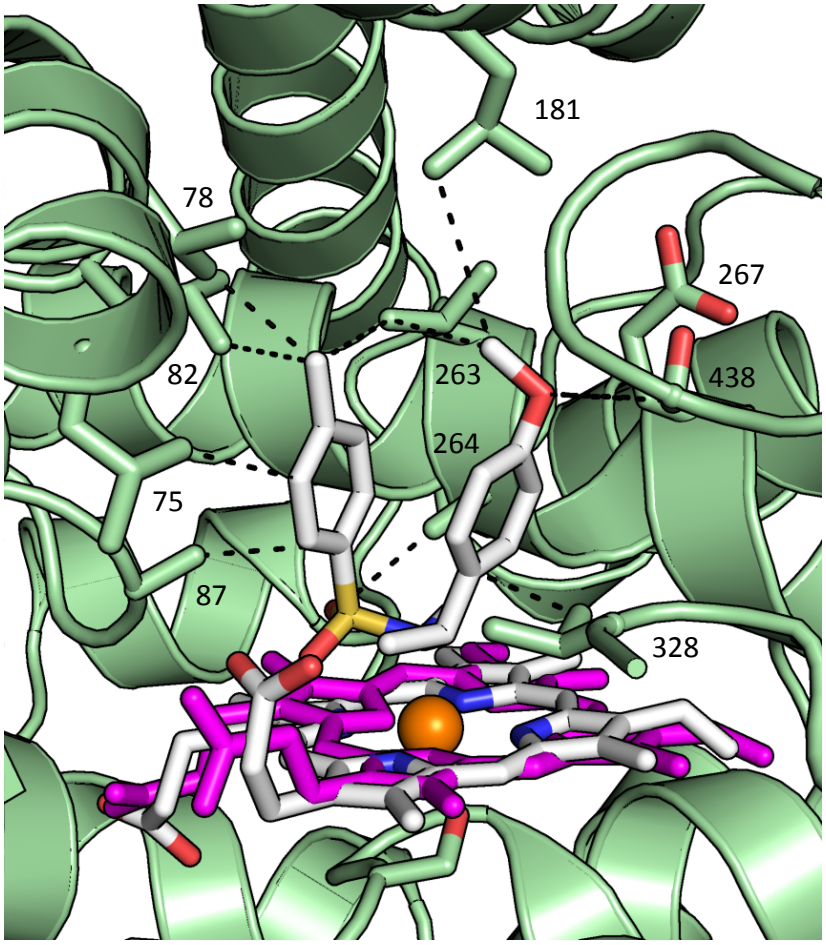

Supplementary Figure 8. Docking of the (*R*)-**4**/heme complex into the active site of P411 variant P-4 A82L A78V F263L, second binding mode. The docked ligand is shown in white; the orientation of the heme in the crystal structure is shown in magenta. Distances of closest contact between the ligand and active site residues are shown as black dashes.

Supplemental References

1. de Nanteuil, F., Waser, J. Catalytic [3+2] Annulation of Aminocyclopropanes for the Enantiospecific Synthesis of Cyclopentylamines. *Angew. Chem. Int. Ed*. **50**, 12075–12079 (2011).
2. Kille, S., Acevedo-Rocha, C. G., Parra, L. P., Zhang, Z.-G., Opperman, D. J., Reetz, M. T., Acevedo J. P. Reducing Codon Redundancy and Screening Effort of Combinatorial Protein Libraries Created by Saturation Mutagenesis. *ACS Synth. Biol*. **2**, 83–92 (2013).
3. Gibson, D. G., Young, L., Chuang, R.-Y., Venter, J. C., Hutchinson III, C. A., Smith, H. O. Enzymatic assembly of DNA molecules up to several hundred kilobases. *Nature Methods* **6**, 343–345 (2009).
4. Vatsis, K. P., Peng, H.-M., Coon, M. J. Replacement of active-site cysteine-436 by serine converts cytochrome P450 2B4 into an NADPH oxidase with negligible monooxygenase activity. *J. Inorg. Biochem*. **91**, 542–553 (2002).
5. Fuhrhop, J.-H., Smith, K. M. *Laboratory methods in porphyrin and metalloporphyrin research*. (Elsevier, 1975).
6. Hyster, T. K., Farwell, C. C., Buller, A. R., McIntosh, J. A., Arnold, F. H. Enzyme-Controlled Nitrogen-Atom Transfer Enables Regiodivergent C–H Amination. *J. Am. Chem. Soc*. **136**, 15505–15508 (2014).
7. Farwell, C. C., Zhang, R. K., McIntosh, J. A., Hyster, T. K., Arnold, F. H. Enantioselective Enzyme-Catalyzed Aziridination Enabled by Active-Site Evolution of a Cytochrome P450. *ACS Cent. Sci*. **1**, 89–93 (2015).
8. Bordeaux, M., Singh, R., Fasan, R. Intramolecular C(sp^3)–H amination of arylsulfonyl azides with engineered and artificial myoglobin-based catalysts. *Bioorg. Med. Chem*. **22**, 5697–5704 (2014).
9. Kan, S. B. J.; Lewis, R. D.; Chen, K.; Arnold, F. H. Directed evolution of cytochrome c for carbon–silicon bond formation: Bringing silicon to life. *Science* **354**, 1048–1051 (2016).
10. Takeda, Y., Hayakawa, J., Yano, K., Minakata, S. Transition-metal-free Benzylic C–H Bond Intermolecular Amination Utilizing Chloramine-T and I_2. *Chem. Lett*. **41**, 1672–1674 (2012).

11. Nishimura, T., Yasuhara, Y., Hayashi, T. Asymmetric Addition of Dimethylzinc to *N*-Tosylarylimines Catalyzed by a Rhodium-Diene Complex toward the Synthesis of Chiral 1-Arylethylamines. *Org. Lett*. **8**, 979–981 (2006).
12. Taylor, J. G., Whittall, N., Hii, K. K. Copper-Catalyzed Intermolecular Hydroamination of Alkenes. *Org. Lett*. **8**, 3561–3564 (2006).
13. Albone, D. P., Challenger, S., Derrick, A. M., Fillery, S. M., Irwin, J. L., Parsons, C. M., Takada, H., Taylor, P. C., Wilson, D. J. Amination of ethers using chloramine-T hydrate and a copper(I) catalyst. *Org. Biomol. Chem*. **3**, 107–111 (2005).
14. Harden, J. D., Ruppel, J. V., Gao, G.-Y., Zhang, X. P. Cobalt-catalyzed intermolecular C–H amination with bromamine-T as nitrene source. *Chem. Commun*. 4644–4646 (2007).
15. Molander, G. A., Fleury-Brégeot, N., Hiebel, M.-A. Synthesis and Cross-Coupling of Sulfonamidomethyltrifluoroborates. *Org. Lett*. **13**, 1694–1697 (2011).
16. Ankner, T., Hilmersson, G. Instantaneous deprotection of tosylamides and esters with SmI_2/Amine/Water. *Org. Lett*. **11**, 503–506 (2009).
17. Guijarro, D., Pablo, O., Yus, M. Asymmetric synthesis of chiral primary amines by transfer hydrogenation of N-(*tert*-butanesulfinyl)ketimines. *J. Org. Chem*. **75**, 5265–5270 (2010).
18. Kurita, T., Hattori, K., Seki, S., Mizumoto, T., Aoki, F., Yamada, Y., Ikawa, K., Maegawa, T., Monguchi, Y., Sajiki, H. Efficient and Convenient Heterogeneous Palladium-Catalyzed Regioselective Deuteration at the Benzylic Position. *Chem. Eur. J*. **14**, 664–673 (2008).
19. Kabsch, W. *XDS*. *Acta Crystallographica Section D-Biological Crystallography* **66**, 125–132 (2010).
20. Evans, P. R., Murshudov, G. N. How good are my data and what is the resolution? *Acta Crystallographica Section D-Biological Crystallography* **69**, 1204–1214 (2013).
21. Emsley, P., Cowtan, K. *Coot:* model-building tools for molecular graphics. *Acta Crystallographica Section D-Biological Crystallography* **60**, 2126–2132 (2004).
22. Winn, M. D., Murshudov, G. N., Papiz, M. Z. Macromolecular TLS Refinement in REFMAC at Moderate Resolutions. *Methods Enzymol.* **374**, 300–321 (2003).
23. Painter, J., Merritt, E. A. *TLSMD* web server for the generation of multi-group TLS models. *J. Appl. Cryst.* **39**, 109–111 (2006).

24. Chen, V. B., Arendall III, W. B., Headd, J. J., Keedy, D. A., Immormino, R. M., Kapral, G. J., Murray, L. W., Richardson, J. S., Richardson, D. C. *MolProbity:* all-atom structure validation for macromolecular crystallography. *Acta Crystallographica Section D-Biological Crystallography* **66**, 12–21 (2010).

25. Haines, D. C., Tomchick, D. R., Machius, M., Peterson, J. A. Pivotal Role of Water in the Mechanism of P450BM-3. *Biochemistry* **40**, 13456–13465 (2001).

26. Li, H., Poulos, T. L. The structure of the cytochrome p450BM-3 haem domain complexed with the fatty acid substrate, palmitoleic acid. *Nature Struct. Biol*. **4**, 140-146 (1997).

27. Dundas, J., Ouyang, Z., Tseng, J., Binkowski, A., Turpaz, Y., Liang, J. CASTp: computed atlas of surface topography of proteins with structural and topographical mapping of functionally annotated residues. *Nucl. Acids Res.* **34**, W116–W118 (2006).

28. Trott, O., Olson, A. J. Autodock Vina: Improving the Speed and Accuracy of Docking with a New Scoring Function, Efficient Optimization, and Multithreading. *J. Comput. Chem*. **31**, 455–461 (2010).

29. Mahy, J. P., Battioni, P., Mansuy, D., Fisher, J., Weiss, R., Mispelter, J., Morgenstern-Badarau, I., Gans, P. Iron Porphyrin–Nitrene Complexes: Preparation from 1,1-Dialkylhydrazines. Electronic structure from NMR, Mössbauer, and Magnetic Susceptibility Studies and Crystal Structure of the [Tetrakis(*p*-chlorophenyl)porphyrinato][(2,2,6,6-tetramethyl-1-piperidyl)nitrene]iron Complex. *J. Am. Chem. Soc*. **106**, 1699–1706 (1984).

30. Scott, E. E., White, M. A., He, Y. A., Johnson, E. F., Stout, C. D., Halpert, J. R. Structure of Mammalian Cytochrome P450 2B4 Complexed with 4-(4-Chlorophenyl)imidazole at 1.9-Å Resolution. *J. Biol. Chem*. **279**, 27294–27301 (2004).

31. Poulos, T. L. Cytochrome P450. *Curr. Opin. Struct. Biol*. **5**, 767–774 (1995).